

THE DISTRIBUTION OF EXTRA-GALACTIC NEBULAE¹

By EDWIN HUBBLE

ABSTRACT

The *object* of the investigation is to determine the distribution of extra-galactic nebulae to a faint uniform limiting magnitude. The *material* consists of counts of about 44,000 nebulae on 1283 plates with the 100-inch and 60-inch reflectors, distributed over the three-quarters of the sky north of -30° Dec. The counts are reduced to the standard conditions of excellent one-hour exposures at the zenith on Eastman 40 plates with the 100-inch reflector.

In general no nebulae are found along the Milky Way. The *zone of avoidance*, representing local obscuration, is irregular and follows the general pattern of the known obscuring clouds. It is bordered by partial obscuration, which fades away into the regions of *normal distribution* where the frequency-curve of $\log N_m$ closely approximates a Gaussian error-curve.

Systematic *variations in longitude* are appreciable only in the lower latitudes, where obscuration appears to be conspicuously greater in the direction of the galactic center than in the opposite direction. There is a definite variation with *latitude*, which from the poles to about $\beta = 15^{\circ}$ is represented by the *cosecant formula*

$$\log N_m = C - 0.15 \operatorname{cosec} \beta ,$$

indicating a total obscuration of 0.5 mag. from pole to pole with *no appreciable difference* between the two hemispheres.

With allowance for the effect of the red shift, the rate of increase of $\log N$ with exposure time suggests *uniform distribution in depth*.

The standard conditions represent a *threshold of identification* for nebulae at about 20.0 pg m. Corrected for red shift, the *number of nebulae* per square degree to magnitude m is

$$\log N_m = 0.6m - 9.12 ,$$

which leads to values for the *density of matter in space* of $\log \rho = -16.4$ to -16.8 in nebulae per cubic parsec, or -29.8 to -29.9 gr/cc, depending upon the value adopted for the mean absolute magnitude of nebulae.

PART I. RELATIVE DISTRIBUTION OF NEBULAE OVER THE SKY

The empirical approach to the problem of the structure of the physical universe consists in extrapolating the observed characteristics of the sample available for inspection. If the sample is fair and the characteristics are well determined, the method may be significant. Investigations have recently emerged from the stellar system and now range through a large volume of space whose inhabitants, the nebulae, are of the same general order as the stellar system itself. There are as yet no indications of a super-system of nebulae analogous to the system of stars. Hence, for the first time, the region now

¹ *Contributions from the Mount Wilson Observatory, Carnegie Institution of Washington*, No. 485.

observable with existing telescopes may possibly be a fair sample of the universe as a whole. This circumstance enhances the interest in, and possibly the value of, the determination of general characteristics.

The first reliable information concerning extra-galactic regions came from stars involved in the nearer nebulae, which provided rough methods of estimating distances—clues which have been rapidly exploited during the last decade until now we have a hasty sketch of some of the general features of the observable region as a unit. The next step was to follow the reconnaissance with a survey—to repeat carefully the explorations with an eye to accuracy and completeness. The program, with its emphasis on methods, will be a tedious series of successive approximations, but the procedure is necessary, since extrapolations beyond the frontiers will be significant only in proportion to the accuracy with which the trend of correlations has been established out to the frontier itself.

The present discussion is a contribution to the program in the form of an investigation of nebular distribution as observed with the large reflectors at Mount Wilson. The purpose is to delimit more closely the influence of local galactic obscuration and to sketch out the general background of normal distribution against which irregularities, local or systematic, may be further investigated. Few of the results are wholly new, but they are formulated more precisely than has hitherto been possible, in keeping with the character of the investigation as a second approximation toward the end in view.

Unless otherwise stated, the term “nebula” is used throughout the discussion to designate the extra-galactic nebulae alone. Latitude and longitude refer to galactic co-ordinates and are designated by β and λ , respectively.²

RECENT CONTRIBUTIONS TO THE SUBJECT

The first modern note in discussions of nebular distribution is found in an article by Hinks³ published in 1911, urging the desira-

² The galactic co-ordinates are referred to the pole at R.A. = 12^h40^m; Dec. +28° (1900). The conversions from equatorial co-ordinates were made or checked with the aid of the tables by John Ohlsson (*Annals of the Observatory at Lund*, No. 3, 1932).

³ A. R. Hinks, *Monthly Notices of the Royal Astronomical Society*, 71, 588, 1911. The earlier literature on the subject is briefly summarized by Hinks.

bility of investigating the nebulae recorded on the Franklin-Adams plates. The gaseous nebulae, both planetary and diffuse, are recognized as galactic in the sense that they concentrate along the Milky Way. The complementary group, "the so-called white nebulae of which the large and better known examples are spirals," are called extra-galactic because

in general they avoid the actual Milky Way zone. But they do it without imposing upon themselves symmetry in either galactic latitude or galactic longitude, and these results suggest that it will be prudent in the future to discuss spiral nebula distribution more on its own merits, and less with an eye to the galactic poles.

The data from the Franklin-Adams plates compiled by Hardcastle⁴ and Fath's⁵ study of plates of Selected Areas with the 60-inch reflector at Mount Wilson, both published in 1914, tended to confirm Hinks's conclusions. Curtis⁶ discussion of nebulae on the Crossley plates at Mount Hamilton contributed

the valuable indication that the density of small nebulae persists to at least 60° from the galactic poles, with only a comparatively small diminution of the frequency of distribution which obtains about the two galactic poles.

This conclusion was confirmed and developed as far as the data permitted in Seares's⁷ very thorough analysis of Fath's counts, published in 1925. In addition, Seares found suggestions of a complicated distribution in longitude with a band of high frequency apparently crossing the northern hemisphere in longitudes 50°–220°.

Wirtz,⁸ in 1923–1924, discussed nebular distribution as indicated by the NGC, by the counts of Fath and of Curtis, and by his own extensive measures of surface brightness. He found no conspicuous dependence of surface brightness on latitude, but some indications of such a dependence on nebular density, in addition to the familiar concentration near the north pole. He concluded that distribution purely according to latitude is only a rough approximation. Well-defined centers of clustering are conspicuous, one of which is near the

⁴ *Monthly Notices of the Royal Astronomical Society*, **74**, 699, 1914.

⁵ *Astronomical Journal*, **28**, 75, 1914.

⁶ *Publications of the Lick Observatory*, **13**, 11, 1918.

⁷ *Mt. Wilson Contr.*, No. 297; *Astrophysical Journal*, **62**, 168, 1925.

⁸ *Astronomische Nachrichten*, **222**, 33, 1924; **223**, 123, 1924; also *Meddelanden från Lunds Astron. Observatorium*, Ser. II, No. 29, 1923.

north pole. The fainter the nebulae, however, the less pronounced the concentration toward the pole and the more defined the tendency toward uniform distribution over the sphere.

Reynolds,⁹ in 1923, discussed the distribution of the brighter nebulae and called attention, among other items, to apparent anomalies in the distribution in longitude. For instance, the large spirals and the globular star clusters tend to be mutually exclusive, congregating in opposite hemispheres whose poles are near the galactic plane. Moreover, he stated, "there is very definite evidence of a band, fairly widespread in the Ursa Major region, stretching past the pole beyond Virgo, the average size becoming smaller as the band passes beyond the pole."

The band is in the general region of that later suggested by Seares and represents the phenomenon described much earlier as the Milky Way of the nebulae.

Provisional results from the present survey were summarized¹⁰ in 1931. Although the quantitative results have been revised in the present more detailed analysis, the general outlines of the picture remain unchanged and need not be restated.

In 1932 appeared the Harvard¹¹ survey of nebulae brighter than the thirteenth magnitude, which covers the entire sky in a homogeneous manner. The results concerning distribution were summarized as "the avoidance of low latitudes, the strong clustering in the northern galactic hemisphere, and the general unevenness of distribution." Later, in 1933, Shapley¹² discussed the distribution of nebulae to much fainter limits on the basis of approximately 100,000 nebulae photographed with the Bruce 24-inch refractor, stating that "there is no change with latitude north of $+25^\circ$; south of -25° the mean density increases, but the obstructing streamers of dark nebulosity in latitude -20° to -40° are probably largely responsible for the apparent increase." He further emphasized the apparent irregularities in distribution and the greater richness in the northern hemisphere.

⁹ *Monthly Notices of the Royal Astronomical Society*, **83**, 147, 1922; **84**, 76, 1923.

¹⁰ *Publications of the Astronomical Society of the Pacific*, **43**, 282, 1931; also *Science*, **75**, 24, 1932, and *Annual Report of the Mount Wilson Observatory*, 1930, 1931, and 1932.

¹¹ Shapley and Ames, *Harvard Annals*, **88**, Part II, 1932.

¹² *Proceedings of the National Academy of Sciences*, **19**, 389, 1933.

THE OBSERVATIONAL DATA FOR THE INVESTIGATION

With the broad features of nebular distribution thus outlined, it was evident that further reliable information could be expected only from large bodies of new data, reasonably complete and thoroughly homogeneous. An examination of the reflector plates available at Mount Wilson in 1926 proved them unsuitable for the particular purpose, owing to lack of uniformity in aperture, emulsion, development, exposure, distribution, etc. A special survey was therefore initiated, and current programs of direct photography were modified where possible to meet the new requirements. Extensive studies of threshold images were also undertaken, with especial attention to the comparison of plates taken with various instruments and under various exposure conditions, until now it is believed that a consistency has been attained in the treatment of nebular images which warrants a general discussion of the accumulated material.

At present about eighty thousand nebulae have been identified on Mount Wilson photographs, of which some sixty thousand are on plates in the writer's collection. Of the latter, about three-fourths¹³ were observed under the standard conditions adopted for the present investigation. Both reflectors are represented indiscriminately, but, owing to differences in mounting, the 100-inch alone is generally used south of about -20° Dec., and the 60-inch alone north of about $+60^{\circ}$.

The standard conditions were Newtonian foci, full apertures, Eastman 40 plates— 5×7 inches for the 100-inch and 4×5 inches for the 60-inch, and full development with a hydroquinone developer (X-ray). Minor variations in sky, mirrors, emulsions, and development were treated as accidental errors, but corrections were applied for atmospheric extinction, variations in definition, and exposure time. The nebular counts were first reduced to the equivalent of one-hour exposures, of excellent definition, at the zenith, with the 100-inch, and in this form were used for the investigation of relative distribution. Later the results were reduced to numbers of nebulae per square degree to a definite limiting magnitude for the purpose of

¹³ The residue are about equally divided among plates of the great clusters; plates with the Ross correcting lens; plates with other apertures, emulsions, or development; and plates with the 10-inch camera.

deriving significant quantitative values for various characteristics of the observable region.

Each plate was examined at least three times with high and low power, the last examination being a continuous review of the entire collection in the light of accumulated experience for the purpose of improving the consistency of the counts and the estimates of quality. All images not definitely stars or obvious defects were marked as nebulae. Comparisons of pairs of duplicate plates indicate that mistakes tend to balance misses; hence, for statistical purposes, the counts appear to be fairly homogeneous.¹⁴

It is impossible, however, to identify all nebulae recorded on a plate from the appearance of the images alone. Numbers increase rapidly with diminishing size and brightness, and, in the faintest half-magnitude, where about one-half of the total may be expected, the nebulae tend to lose themselves among the stars. The threshold of identification varies with the type; open spirals fade out, while areas are still perceptible, and compact globular nebulae merge into the star images well above the limit of the plates. This effect can be treated as statistically uniform, since it depends upon the relative frequencies of nebular types and there is no reason to assume that the relations vary systematically over the sky. But the threshold of identification also varies with the criteria upon which different observers, consciously or unconsciously, base their judgments. This irregularity represents a personal equation which may attain consider-

¹⁴ The accuracy of the counts was tested in various ways. Several dozen duplicates were included in the collection, but most of them represent plates discarded for particular reasons (usually poor seeing) and replaced by others of better quality. Fifteen duplicates, however, were judged suitable for comparison purposes, and these pairs of independent counts, when reduced to the standard system, show an average difference without regard to sign of about 0.05 in $\log N$. Some of the difference can be attributed to uncertainties in the reduction, especially in the corrections for quality, which exhibit a considerable range.

A more detailed investigation of these fifteen pairs (six with the 60-inch, four with the 100-inch, and five with both telescopes), together with eight two-hour exposures with the 100-inch (not included in the discussion), of fields covered by hour exposures with either telescope, indicated that among about 1020 identifications on plates included in the survey, 42 were mistakes representing defects and stars, while 56 nebulae were missed, although above the threshold of identification. A ratio of this order is assumed to hold for the entire body of data. The relative number of nebulae actually recorded, but below the threshold of identification, is discussed later.

able proportions and must be calibrated before counts by various observers can be compared. The personal equation may also be expressed as the difference between the limiting magnitude of the nebular counts and the limiting magnitude of the star images on the plates—a quantity which varies with the observer as well as the instrumental equipment. Calibration of the present counts has been attempted in some detail, since the writer believes that the interpretation of most of the published counts is seriously restricted or even confused by the omission of this important feature.

The observational data, together with $\log N$ reduced to a homogeneous system, are listed in Tables I–IV.

Table I gives the survey data. The 765 plates, about equally divided between the two reflectors, are distributed along circles of latitude 5° apart, the galactic equator itself being omitted. From $\beta = 5^\circ$ to 60° , the longitude intervals are 10° ; for $\beta = 65^\circ$ and 70° , the intervals are 20° ; for $\beta = 75^\circ$ and 80° , they are 30° ; for $\beta = 85^\circ$, they are 60° . With the exception of six fields,¹⁵ the survey is complete to Dec. = -30° and hence covers three-fourths of the sphere, including both galactic poles and about two-thirds of the Milky Way. The northern hemisphere is complete from the pole to and including $\beta = +40^\circ$. The corresponding southern cap, $\beta = -40^\circ$ to -90° , is about 60 per cent complete.

Uniform exposures of one hour were used for 690 plates, and half-hour exposures for 74 plates scattered along the latitude circles at $\beta = 35^\circ, 45^\circ, 55^\circ$, and 65° . The half-hour exposures, which are marked with an asterisk in Table I, were included primarily for use in determining the manner in which numbers of nebulae increase with exposure time. For the same reason a 45-minute exposure was included and marked with a double asterisk. The last column of the table gives the values of $\log N$ reduced to the uniform conditions of one-hour exposures of excellent quality at the zenith with the 100-inch. $\log N$ is simply the sum of $\log N_r$ (the number of nebulae ac-

¹⁵ The exceptions are $\beta = +20^\circ, \lambda = 310^\circ$; $-25^\circ, 200^\circ$; $-45^\circ, 190^\circ$; $-55^\circ, 190^\circ$; $-65^\circ, 190^\circ$, and 350° . The plates were rejected for various reasons and attempts to repeat them have failed. Counts on the rejected plates are considered uncertain, but they indicate no remarkable deviations from normal distribution; hence their omission is not very material.

TABLE I*
SURVEY FIELDS

β	λ		Z	Q	N_1	I	log N	β	λ		Z	Q	N_1	I	log N
+90°	h	39°	E	71	6	1.90	+65°	140°	s*	7°	E	14	2	1.71
85	0°	h	29	FG	60	7	1.98	160°	s*	19	GE	14	2	1.76	
	60	h	20	E	50	2	1.71	180°	h	32	F	37	5	1.88	
	120	h	41	E	37	3	1.63	200°	s	19	E	67	6	2.00	
	180	h	34	F	80	4	2.22	220°	s	30	E	84	12	2.11	
	240	h	15	E	51	4	1.71	240°	h*	28	E	26	2	1.83	
	300	h	11	E	60	10	1.78	260°	s	32	FG	36	4	1.93	
80	0	h	11	FG	41	4	1.79	280°	h	34	GE	48	4	1.76	
	30	s	51	G	44	5	2.00	300°	h*	33	F	11	2	1.75	
	60	s	41	E	43	9	1.85	320°	h	33	GE	86	5	2.00	
	90	s	42	FG	23	5	1.76	340°	s*	17	E	16	1	1.77	
	120	s	37	F	19	1	1.76	60	0	s	21	E	58	12	1.93
	150	s	39	E	77	7	2.10	10	s	28	G	54	4	2.01	
	180	h	23	GE	54	5	1.78	20	s	42	G	35	5	1.86	
	210	s	55	G	32	7	1.90	30	s	13	GE	39	6	1.79	
	240	h	43	FG	44	4	1.88	40	s	43	F	14	2	1.65	
	270	h	41	G	62	5	1.95	50	s	19	G	31	5	1.76	
	300	h	49	G	72	5	2.05	60	s	18	G	28	4	1.72	
	330	s	43	GE	76	9	2.14	70	s	37	G	25	3	1.70	
75	0	h	34	E	90	10	1.99	80	s	32	G	46	6	1.95	
	30	s	16	E	58	10	1.93	90	s	24	GE	40	1	1.81	
	60	s	7	F	22	1	1.78	100	s	42	GE	79	14	2.16	
	90	s	34	E	54	6	1.93	110	s	21	GE	85	12	2.14	
	120	s	23	E	30	7	1.65	120	s	30	GE	31	2	1.72	
	150	s	29	E	39	2	1.77	130	h	43	FG	52	8	1.96	
	180	h	8	E	97	9	1.99	140	s	30	G	31	6	1.78	
	210	h	32	GE	67	2	1.90	150	h	26	GE	145	23	2.22	
	240	s	30	G	83	5	2.21	160	h	28	GE	37	3	1.63	
	270	h	35	GE	63	7	1.88	170	h	7	GE	37	9	1.61	
	300	h	33	E	73	12	1.90	180	h	34	FG	50	5	1.92	
	330	h	22	FP	27	2	1.89	190	h	17	GE	64	8	1.86	
70	0	s	43	G	44	5	1.96	200	s	45	F	31	3	2.00	
	20	h	39	G	43	4	1.78	210	h	29	E	120	8	2.10	
	40	s	28	F	31	5	1.95	220	s	36	E	67	13	2.03	
	60	s	34	G	29	2	1.76	230	h	41	E	88	7	2.00	
	80	h	41	G	76	7	2.04	240	s	37	E	36	6	1.76	
	100	h	41	G	36	6	1.72	250	h	40	GE	77	7	1.98	
	120	s	26	G	51	2	1.99	260	h	36	GE	41	5	1.69	
	140	s	44	GE	44	6	1.91	270	s	42	E	77	10	2.11	
	160	s	35	E	52	12	1.92	280	s	46	GE	34	2	1.81	
	180	s	20	FG	36	7	1.91	290	s	45	E	76	12	2.11	
	200	s	37	E	69	3	2.04	300	s	33	GE	35	6	1.77	
	220	s	49	FG	33	3	1.95	310	h	50	G	65	7	2.01	
	240	h	33	GE	75	8	1.95	320	s	36	GE	53	9	1.96	
	260	h	37	FG	43	5	1.85	330	h	52	FG	56	7	2.04	
	280	h	38	G	35	1	1.69	340	s	20	GE	74	9	2.08	
	300	h	37	FG	44	5	1.86	350	s	43	G	35	3	1.86	
	320	h	29	FG	40	4	1.80	+55	0	h*	25	E	39	5	2.01
	340	h	21	G	38	5	1.71	10	s	8	GE	380	32	2.78	
+65	0	s*	13	E	18	5	1.82	20	s*	17	E	20	2	1.87	
	20	s*	19	E	12	1	1.65	30	s*	25	E	16	1	1.78	
	40	s*	19	E	17	3	1.80	40	s*	25	GE	17	3	1.85	
	60	s*	23	E	12	0	1.65	50	s*	23	GE	16	3	1.81	
	80	s*	10	F	13	1	1.95	60	s*	25	GE	22	2	1.96	
	100	s	35	E	51	3	1.91	70	s*	43	E	37	6	2.19	
	120	s*	14	E	17	3	1.79	80	s	35	GE	57	8	2.00	
								90	s*	29	F	7	1	1.71	
								100	s	39	GE	58	5	2.01	
								110	s*	26	E	33	5	2.10	

* Symbols are: β , λ =galactic latitude and longitude; "h"=100-inch, "s"=60-inch, Z=zenith distance at mid-exposure, Q=quality of plate, N_1 =number of nebulae actually counted, I=number within central circle (diameter 10' for 100-in., 13'8 for 60-in.); corrections from Tables VI, VII, and IX, added to log N_1 , give log N, N being the number of nebulae for an hour's exposure of excellent quality at the zenith with the 100-inch. All exposures are 60^m except those for which "h" or "s" are starred. A single star indicates a 30^m exposure and a double star (one field only, $\beta = +55^\circ$, $\lambda = 130^\circ$), a 45^m exposure.

Two fields of quality P ($\beta = +35^\circ$, $\lambda = 300^\circ$; $\beta = -15^\circ$, $\lambda = 140^\circ$) are included for which the quality factor, $\Delta Q = 0.70$, is not evaluated in the text but represents a result of low weight indicated by a dozen rejected P plates.

TABLE I—Continued

β	λ		Z	Q	N_i	I	log N	β	λ		Z	Q	N_i	I	log N		
+55°	120°	s*	23°	F	13	1	1.96	+45°	110°	s*	33°	F	11	0	1.91		
	130	s	16	GE	19	3	1.66		120	s*	27	E	30	3	2.06		
	140	s*	14	E	15	4	1.74		130	s*	21	GE	27	6	2.04		
	150	s*	16	G	10	4	1.67		140	s*	15	FG	15	3	1.92		
	160	s*	16	G	14	3	1.82		150	s*	12	E	26	3	1.97		
	170	h	10	F	33	8	1.80		160	s*	11	E	16	3	1.76		
	180	s	33	GE	53	7	1.95		170	h	27	FP	23	1	1.83		
	190	s	25	GE	59	9	1.99		180	s*	17	E	16	3	1.77		
	200	h	22	G	76	8	1.99		190	h	27	F	30	4	1.78		
	210	s	28	GE	44	4	1.86		200	h*	28	GE	21	1	1.78		
	220	h	34	FP	31	4	1.98		210	s*	35	G	31	6	2.19		
	230	s*	34	E	27	1	2.03		220	s	43	E	31	5	1.71		
	240	s*	42	F	8	0	1.80		230	s*	44	F	7	2	1.76		
	250	s*	40	E	32	2	2.12		240	s*	48	G	15	2	1.93		
	260	s	47	GE	17	2	1.91		250	s*	49	G	11	2	1.79		
	270	s	41	GE	75	14	2.14		260	s*	51	FG	9	3	1.79		
	280	s	42	GE	77	9	2.15		270	s	51	GE	48	3	1.98		
	290	h*	41	FG	15	0	1.82		280	s	51	GE	31	1	1.79		
	300	s	40	FG	35	3	1.93		290	s*	49	GE	20	5	1.99		
	310	h*	36	G	22	2	1.88		300	h	47	FG	26	4	1.67		
	320	s	31	GE	75	6	2.11		310	h	48	G	42	6	1.81		
	330	h*	30	GE	35	3	2.01		320	h	50	FG	36	2	1.84		
	340	s	28	GE	72	9	2.08		330	h	42	FG	48	4	1.92		
	350	h*	23	G	21	4	1.83		340	h	38	GE	110	9	2.13		
									350	h*	42	G	20	2	1.86		
	50	0	h	14	FG	66	8		2.00	40	0	h	29	F	50	6	2.00
		10	h	19	G	60	6		1.89		10	h	40	F	44	6	1.97
		20	h	31	FG	61	3		2.00		20	h	35	FG	50	3	1.97
		30	s	14	G	22	1		1.60		30	s	17	G	44	4	1.91
		40	s	17	G	33	4		1.79		40	s	13	GE	37	7	1.77
		50	s	35	G	38	1		1.88		50	s	25	GE	48	9	1.90
		60	s	37	E	30	1		1.68		60	s	30	GE	24	2	1.61
		70	s	36	G	33	2		1.82		70	s	38	FG	24	4	1.77
		80	s	41	GE	22	3		1.60		80	s	41	GE	34	8	1.79
		90	s	41	G	40	5		1.92		90	s	44	FG	45	4	2.06
100		s	37	G	23	2	1.66	100	s		42	FG	21	2	1.72		
110		s	41	GE	32	2	1.77	110	s		38	E	50	7	1.91		
120		s	45	GE	36	3	1.83	120	s		34	G	32	6	1.81		
130		s	35	GE	58	12	2.00	130	s		26	E	77	15	2.07		
140		s	22	GE	29	2	1.67	140	s		25	FP	21	5	1.93		
150		h	37	F	26	2	1.73	150	s		8	F	32	5	1.95		
160		h	23	FP	29	1	1.92	160	h		31	G	107	23	2.16		
170		h	26	F	49	7	1.99	170	s		31	GE	47	6	1.90		
180		h	21	FG	53	5	1.91	180	h		48	F	31	2	1.86		
190		h	37	FP	23	4	1.85	190	h		50	F	24	4	1.76		
200		h	25	F	35	7	1.84	200	s		42	F	28	9	1.95		
210		s	35	G	84	16	2.22	210	s		45	G	91	15	2.20		
220		s	40	GE	42	4	1.87	220	h		43	FG	95	11	2.22		
230		s	40	GE	41	4	1.86	230	h		51	FP	23	4	1.91		
240		s	47	GE	32	3	1.79	240	h		52	F	16	1	1.59		
250	s	44	GE	28	5	1.72	250	h	54	FG	31	5	1.79				
260	s	47	FG	21	1	1.74	260	h	56	FG	25	1	1.72				
270	s	50	G	37	7	1.93	270	h	57	FG	61	7	2.12				
280	s	43	GE	24	5	1.64	280	h	56	FG	34	1	1.85				
290	h	47	F	40	4	1.96	290	h	54	FG	46	4	1.96				
300	h	43	F	51	7	2.05	300	h	52	FG	48	2	1.97				
310	h	40	FP	19	0	1.78	310	h	48	FG	27	4	1.70				
320	h	46	F	32	5	1.87	320	h	43	FG	48	6	1.92				
330	h	34	FP	22	0	1.83	330	h	37	FP	13	3	1.60				
340	h	31	F	45	3	1.96	340	h	43	FP	10	1	1.51				
350	h	39	FP	32	1	2.01	350	s	34	E	37	5	1.77				
+45	0	h*	45	G	42	0	2.10	+35	0	h	32	G	30	0	1.61		
	10	h	15	E	65	13	1.81		10	h	16	GE	55	3	1.79		
	20	h	3	GE	07	10	1.87		20	h	5	GE	30	4	1.52		
	30	h	29	GE	72	6	1.92		30	s	18	GE	43	4	1.84		
	40	s	21	G	50	5	1.97		40	s	23	FG	17	2	1.58		
	50	s	35	GE	94	7	2.21		50	s	27	FG	9	1	1.31		
	60	s	48	G	39	7	1.94		60	s	30	F	24	2	1.81		
	70	s	53	FG	25	5	1.86		70	s	39	GE	33	5	1.77		
	80	s	52	F	17	3	1.78		80	s	44	G	22	2	1.67		
	90	s	41	FP	20	2	1.80		90	s	51	GE	43	6	1.93		
	100	s*	39	E	50	5	2.31										

THE DISTRIBUTION OF EXTRA-GALACTIC NEBULAE 17

TABLE I—Continued

β	λ		Z	Q	N_1	I	log N	β	λ		Z	Q	N_1	I	log N			
+35°	100°	s	47°	GE	47	2	1.95	+25°	110°	s	40°	G	29	5	1.77			
	110	s	43	G	35	3	1.86		120	s	40	G	14	2	1.46			
	120	s	29	FG	31	4	1.85		130	s	26	G	31	7	1.74			
	130	s	26	FG	45	3	2.01		140	s	11	G	37	10	1.83			
	140	s	33	GE	56	7	1.98		150	h	27	G	52	2	1.84			
	150	s	33	GE	82	26	2.14		160	s	23	G	47	10	1.94			
	160	s*	9	GE	60	7	2.38		170	s	16	GE	46	9	1.87			
	170	s	39	GE	52	6	1.97		180	h	30	FG	44	6	1.85			
	180	s	21	E	61	11	1.96		190	h	42	FG	49	8	1.93			
	190	s*	28	E	18	2	1.84		200	h	46	GE	76	6	2.00			
	200	s	39	GE	22	3	1.59		210	h	43	FG	45	7	1.89			
	210	s*	41	GE	19	4	1.94		220	h	56	G	45	7	1.80			
	220	h*	46	GE	21	1	1.84		230	h	59	G	25	5	1.67			
	230	s	51	G	30	3	1.84		240	h	64	F	31	5	2.00			
	240	h*	55	FG	17	3	1.94											
	250	h*	59	F	18	3	2.11		300	h	64	G	14	3	1.48			
	260	h*	62	F	7	0	1.73		310	h	59	GE	11	1	1.25			
	270	h*	62	F	8	1	1.78		320	h	55	G	12	0	1.31			
	280	h*	62	F	31	0	2.37		330	h	48	G	9	1	1.14			
	290	h*	60	FG	44	4	2.40		340	s	42	FG	6	0	1.18			
	300	h	56	P	6	1	1.62		350	s	43	G	10	1	1.32			
	310	s	51	G	39	4	1.95											
	320	s	46	G	8	0	1.24		20	o	h	25	G	14	1	1.27		
	330	s	42	FG	16	5	1.60		10	h	25	GE	32	2	1.63			
	340	s	35	GE	37	3	1.81		20	s	8	GE	21	4	1.52			
	350	s	28	G	30	6	1.76		30	s	31	G	27	4	1.72			
	30	o	h	40	F	32	5		1.84	40	s	35	F	19	3	1.76		
		10	h	42	F	19	1		1.62	50	s	23	GE	22	7	1.55		
		20	h	41	G	40	6		1.76	60	s	29	GE	22	4	1.56		
		30	s	21	FG	17	3		1.58	70	o	0	0	0	0	0	0	
		40	s	32	G	26	2		1.70	80	s	46	G	0	0	0	0	0
		50	s	25	GE	40	15		1.82	90	s	52	FG	7	2	1.30		
		60	s	36	GE	17	1		1.47	100	s	44	FG	8	2	1.23		
		70	s	47	GE	15	1		1.46	110	s	38	FG	23	5	1.75		
		80	s	54	FG	11	3		1.50	120	s	30	G	12	4	1.37		
90		s	53	GE	17	2	1.55	130	s	38	F	16	1	1.69				
100		s	48	F	26	3	1.94	140	s	27	FP	15	2	1.81				
110		s	46	G	32	3	1.85	150	h	10	GE	150	14	2.22				
120		s	36	GE	48	9	1.92	160	h	22	G	49	5	1.80				
130		s	31	GE	64	11	2.04	170	s	26	G	51	4	1.99				
140		h	41	F	44	7	1.98	180	s	25	G	32	3	1.70				
150		s	14	G	35	3	1.80	190	s	44	G	30	7	1.81				
160		h	5	FG	32	4	1.69	200	h	44	G	36	7	1.73				
170		s	33	G	118	16	2.36	210	h	49	F	27	2	1.80				
180		h	30	F	33	5	1.83	220	h	56	F	41	3	2.03				
190		s	29	FG	32	4	1.87	230	h	63	FG	24	1	1.77				
200		g	48	G	45	4	1.84	320	h	56	F	0	0	0	0			
210		h	43	FG	56	9	1.99	330	h	50	F	0	0	0	0			
220		h	49	G	39	7	1.78	340	s	44	FG	0	0	0	0			
230		h	55	FG	24	0	1.69	350	s	43	G	0	0	0	0			
240		h	60	G	16	2	1.48											
250		h	63	F	22	2	1.83	+15	o	h	29	FG	30	3	1.68			
290		h	64	FP	38	2	2.26	10	h	33	FG	14	2	1.36				
300		h	60	F	33	2	1.98	20	s	19	G	18	3	1.53				
310		h	55	FG	16	3	1.51	30	h	19	GG	30	5	1.69				
320		h	50	FG	18	5	1.54	40	s	30	FG	6	0	1.15				
330		h	46	F	15	1	1.54	50	s	44	F	18	3	1.77				
340		h	38	FG	18	2	1.49	60	s	28	G	13	4	1.39				
350		h	38	F	20	4	1.63	70	s	38	F	0	0	0	0			
+25		o	h	27	FG	24	3	1.58	80	s	43	FG	1	0	0.40			
		10	h	30	FG	53	4	1.93	90	s	47	FG	0	0	0			
	20	h	35	FG	29	5	1.68	100	s	40	F	4	0	1.09				
	30	h	47	G	25	2	1.58	110	s	33	G	9	4	1.24				
	40	s	28	F	18	3	1.72	120	s	26	F	4	2	1.06				
	50	s	38	G	27	9	1.74	130	s	31	FG	9	2	1.32				
	60	s	31	FG	23	5	1.73	140	s	19	F	10	1	1.45				
	70	s	41	G	20	4	1.62	150	h	12	G	40	10	1.70				
	80	s	49	G	22	2	1.69	160	h	12	G	43	5	1.73				
	90	s	53	G	10	1	1.38	170	h	36	F	12	1	1.40				
	100	s	46	FG	18	1	1.68	180	h	27	F	30	5	1.78				
								190	h	38	GG	79	13	2.05				
								200	h	45	G	48	3	1.86				

TABLE I—Continued

β	λ		Z	Q	N_1	I	$\log N$	β	λ		Z	Q	N_1	I	$\log N$	
+15°	210°	h	53°	F	11	1	1.44	- 5°	90°	s	23°	G	0	
	220	h	59	F	7	1	1.30		100	s	22	G	2	0	0.57
	320	h	60	FG	0		110	s	24	FG	1	0	0.36
	330	h	58	F	0		120	s	37	G	0
	340	h	47	F	0		130	s	6	G	0
	350	h	47	FG	0		140	h	27	F	0
									150	h	23	G	0
									160	h	50	FG	11	2	1.32
									170	h	28	G	7	0	0.97
									180	h	50	FP	0
10	10	s	25	G	2	1	0.58	190	h	46	GE	0	
	20	h	15	G	7	1	0.95	200	h	55	F	0	
	30	h	21	FG	1	1	0.19	210	h	63	F	2	0	0.79	
	40	h	15	G	44	10	1.74									
	50	s	14	G	22	4	1.60									
	60	s	22	G	0	330	h	64	G	0	
	70	s	34	FG	0	340	h	60	G	0	
	80	s	40	FG	0	350	s	46	F	0	
	90	s	45	G	0									
	100	s	39	G	0	10	o	h	39	F	0
110	s	38	GE	0	10	s	35	G	0		
120	s	26	G	0	20	h	25	G	9	1	1.07		
130	s	41	F	3	1	0.98	30	h	14	G	4	0	0.70		
140	s	25	G	7	0	1.13	40	s	31	G	2	0	0.59		
150	s	34	FG	2	0	0.68	50	h	45	FG	11	0	1.29		
160	h	27	G	7	2	0.97	60	s	21	G	7	1	1.12		
170	h	27	G	10	1	1.12	70	s	26	G	12	4	1.36		
180	h	50	F	3	1	0.86	80	s	28	G	23	4	1.64		
190	h	40	FP	10	0	1.50	90	s	25	FG	0		
200	h	47	G	25	8	1.58	100	s	20	G	9	1	1.22		
210	h	55	F	21	3	1.73	110	s	37	G	17	5	1.53		
220	h	63	FG	3	2	0.87	120	h	50	FG	6	1	1.06		
							130	h	38	F	0		
							140	h	45	F	0		
							150	h	23	F	7	1	1.14		
							160	h	26	G	0		
							170	h	33	G	0		
							180	s	41	G	0		
							190	h	48	FG	0		
							200	h	57	FP	4	1	1.20		
							210	h	65	FP	4	0	1.29		
							340	s	56	FG	0		
							350	s	46	G	0		
							15	o	h	47	FP	16	1	1.73	
							10	h	39	F	3	1	1.67		
							20	h	38	F	10	1	1.33		
							30	s	26	G	10	1	1.28		
							40	s	17	G	9	1	1.22		
							50	s	38	F	4	1	1.09		
							60	h	32	G	39	3	1.72		
							70	s	35	GE	12	0	1.32		
							80	s	18	G	22	3	1.61		
							90	h	48	F	22	1	1.71		
							100	s	19	FG	13	1	1.46		
							110	h	45	FG	74	11	2.12		
							120	h	40	FP	5	0	1.20		
							130	h	31	G	11	1	1.17		
							140	h	14	P	3	0	1.18		
							150	h	18	F	0		
							160	h	29	G	21	4	1.44		
							170	h	43	G	23	2	1.52		
							180	h	44	G	3	1	0.65		
							190	h	50	FP	14	0	1.70		
							200	h	62	FG	44	4	2.02		
							340	h	59	F	0		
							350	s	52	F	1	0	0.55		
							-20	o	h	43	G	16	1	1.36	
							10	h	38	G	20	1	1.45		
							20	h	50	FG	14	0	1.43		
							30	s	39	FG	13	2	1.50		

THE DISTRIBUTION OF EXTRA-GALACTIC NEBULAE 19

TABLE I—Continued

β	λ		Z	Q	N_z	I	$\log N$	β	λ		Z	Q	N_z	I	$\log N$			
-20°	40°	h	33°	GE	13	1	1.18	-35°	30°	h	43°	GE	27	2	1.53			
	50	h	6	FG	12	1	1.26		40	s	25	F	12	0	1.54			
	60	h	31	GE	12	0	1.15		50	s	41	G	27	5	1.75			
	70	h	26	F	11	2	1.34		60	s	27	GE	42	4	1.84			
	80	h	43	F	30	7	1.82		70	h	34	GE	125	11	2.18			
	90	s	16	F	14	3	1.60		80	h	34	GE	52	6	1.80			
	100	h	28	F	45	5	1.95		90	s	14	GE	33	3	1.72			
	110	h	26	FG	36	5	1.76		100	h	45	E	69	5	1.91			
	120	h	25	G	37	7	1.69		110	h	39	GE	29	1	1.55			
	130	h	25	F	9	0	1.25		120	h	33	E	48	4	1.71			
	140	h	19	FG	4	0	0.79		130	h	50	G	40	1	1.80			
	150	h	23	F	1	0	0.20		140	s	39	GE	2	0	0.55			
	160	h	27	G	36	3	1.68		150	h	50	GE	17	3	1.37			
	170	s	41	G	40	5	1.92		160	h	52	GE	39	2	1.74			
	180	h	43	FP	14	3	1.66		170	h	45	F	21	3	1.67			
	190	h	50	FG	75	17	2.16		180	s	49	G	16	2	1.55			
	200	h	61	G	41	6	1.90		190	h	58	FP	18	4	1.87			
		340	h	60	G	6	2		1.06		350	h	57	FG	27	2	1.76	
		350	s	53	GE	9	1		1.26		40	o	s	52	GE	42	11	1.93
	25	o	s	46	GE	18	0		1.54	10	s	45	G	29	5	1.79		
10		s	42	GE	20	2	1.56	20	s	38	E	64	13	2.02				
20		s	43	GE	20	1	1.56	30	s	32	GE	35	8	1.77				
30		s	46	GE	44	6	1.92	40	s	29	E	48	8	1.86				
40		s	21	FG	12	3	1.43	50	s	22	GE	42	8	1.83				
50		s	45	E	33	5	1.75	60	s	23	E	47	3	1.84				
60		s	38	G	17	8	1.54	70	s	17	GE	55	6	2.01				
70		s	27	GE	41	3	1.83	80	s	20	E	61	5	1.96				
80		s	32	GE	22	2	1.57	90	s	15	FG	27	4	1.77				
90		s	36	GE	62	5	2.03	100	s	22	E	75	14	2.05				
100		s	29	E	56	14	1.93	110	s	18	G	35	6	1.81				
110		h	27	F	25	4	1.72	120	s	27	E	45	5	1.83				
120		h	20	GE	51	10	1.76	130	s	26	GE	66	5	2.04				
130		s	50	F	20	3	1.84	140	h	27	FG	6	0	0.98				
140		s	32	FG	6	1	1.15	150	h	57	G	24	2	1.63				
150		h	26	FP	0	0	160	h	52	G	25	2	1.61				
160		h	41	FG	12	2	1.32	170	h	46	GE	70	9	1.97				
170		h	46	FP	20	1	1.83	180	h	54	G	27	3	1.65				
180		h	46	FG	32	2	1.77	190	h	59	G	51	5	1.98				
190		h	50	FG	42	7	1.90		350	h	59	F	20	1	1.75			
	340	h	63	G	13	4	1.42		45	o	h	54	GE	56	6	1.91		
	350	s	55	E	12	3	1.37	10	h*	47	G	14	1	1.73				
30	o	s	48	GE	25	1	1.69	20	h*	41	GE	50	5	2.20				
	10	s	42	GE	25	4	1.66	30	h*	35	GE	16	1	1.68				
	20	s	43	E	16	1	1.42	40	h*	32	E	15	2	1.61				
	30	s	37	E	28	2	1.65	50	h*	35	E	23	2	1.80				
	40	s	38	GE	28	2	1.70	60	h*	30	E	34	8	1.96				
	50	s	20	GE	17	4	1.44	70	h*	21	E	52	5	2.13				
	60	s	10	E	25	2	1.56	80	h	45	G	46	7	1.83				
	70	s	31	GE	31	6	1.72	90	h	36	E	56	3	1.79				
	80	s	14	G	66	5	2.08	100	h	43	E	74	9	1.93				
	90	s	24	G	48	8	1.96	110	h	33	GE	54	5	1.80				
	100	s	15	E	89	11	2.11	120	h	42	G	30	3	1.64				
	110	s	22	G	53	6	1.99	130	h	35	E	67	7	1.87				
	120	s	30	GE	55	19	1.97	140	h	37	GE	21	1	1.46				
	130	s	39	FG	24	5	1.77	150	h	49	E	61	9	1.88				
	140	s	51	F	34	5	2.07	160	h	44	F	67	5	2.18				
	150	h	34	F	21	3	1.64	170	s	48	E	45	6	1.90				
	160	s	38	G	28	6	1.76	180	h	53	F	36	5	1.96				
	170	h	41	FP	16	3	1.71		350	h	60	GE	45	6	1.87			
	180	h	51	FG	29	2	1.74		-50	o	h	56	GE	77	9	2.07		
	190	h	56	F	37	2	1.90	10	h	51	FG	43	4	1.91				
200	h	64	GE	41	2	1.88	20	s	43	F	35	4	2.04					
	340	h	64	G	13	4	1.44	30	h	39	FG	39	4	1.82				
	350	h	57	FP	12	0	1.68	40	s	40	F	28	4	1.94				
-35	o	h	53	FG	21	3	1.62	50	h	33	F	49	7	2.00				
	10	s	50	FG	25	2	1.84	60	s	40	F	28	6	1.94				
	20	h	47	F	22	4	1.70	70	h	43	F	61	5	2.13				

TABLE I—Continued

β	λ		Z	Q	N_1	I	log N	β	λ		Z	Q	N_1	I	log N			
-50°	80°	h	34°	F	25	2	1.72	-60°	190°	h	64°	GE	38	8	1.85			
	90	h	33	FG	21	3	1.53		350	h	64	G	25	4	1.73			
	100	h	37	F	26	2	1.73			65	o	h	60	GE	43	3	1.85	
	110	h	46	FP	22	1	1.87				10	h	56	GE	43	1	1.81	
	120	s	44	GE	65	19	2.08				20	s	51	GE	37	5	1.87	
	130	s	35	F	25	5	1.88				30	s	45	E	49	5	1.92	
	140	s	45	FG	39	5	2.00				40	s	51	GE	36	4	1.86	
	150	h	42	F	51	4	2.05				50	s	43	GE	33	3	1.78	
	160	h	44	FP	24	3	1.90				60	s	40	E	58	10	1.97	
	170	h	51	GE	57	10	1.90				70	h	46	FG	34	4	1.79	
	180	h	56	G	81	6	2.15				80	s*	39	E	21	3	1.93	
	190	h	62	G	29	3	1.76				90	h*	40	FG	39	3	2.22	
	55	350	h	62	GE	45	2				1.89	100	s	39	FG	65	6	2.20
		o	h	59	GE	70	7				2.06	110	h	38	G	32	2	1.66
		10	s	51	GE	47	7				1.97	120	s	41	E	52	2	1.94
		20	h*	41	G	21	1				1.88	130	s	45	GE	30	2	1.75
		30	h*	44	G	34	1				2.10	140	s	40	E	31	5	1.70
		40	h*	40	G	16	1				1.75	150	s	48	E	39	6	1.84
		50	s	34	GE	40	1				1.84	160	s	52	GE	40	7	1.91
60		s*	36	E	14	0	1.75	170			h	56	E	33	4	1.66		
70		s	42	GE	43	7	1.89	180	h		60	F	23	1	1.82			
80		s	36	FG	34	6	1.91	70	o	h	61	FG	47	4	2.04			
90		h*	34	FG	23	2	1.98		20	h	58	G	83	7	2.18			
100		h*	28	F	14	1	1.85		40	h	48	F	26	1	1.78			
110		s	30	E	48	4	1.87		60	h	45	F	43	6	1.98			
120		s	33	E	47	7	1.86		80	h	43	G	61	7	1.95			
130		s	39	E	42	6	1.83		100	h	43	G	68	6	1.99			
140		s	42	E	54	6	1.95		120	h	45	F	43	2	1.98			
150		s	43	GE	32	7	1.77		140	h	51	G	62	8	1.99			
160		s	46	E	45	9	1.89		160	h	54	FG	33	2	1.82			
170		s	52	FG	20	0	1.75		180	h	60	FG	48	8	2.04			
180	h	57	FG	28	3	1.78	75		o	h	61	GE	32	5	1.74			
350	h	63	FG	25	2	1.79			30	s	54	G	34	7	1.91			
o	h	59	FG	52	11	2.07			60	s	49	GE	29	3	1.75			
10	h	53	G	45	5	1.87			90	s	48	G	23	5	1.71			
20	h	49	G	63	8	1.99			120	s	49	E	111	9	2.30			
30	h	45	GE	98	13	2.10			150	h	54	F	27	2	1.83			
40	h	43	E	34	8	1.59			180	h	63	GE	64	3	2.06			
50	s	43	G	32	2	1.83			80	o	h	62	F	45	3	2.13		
60	h	41	F	30	4	1.82				30	h	58	GE	61	8	1.99		
70	s	44	GE	76	11	2.15		60		h	53	G	43	3	1.85			
80	h	34	FP	23	1	1.85		90		h	53	G	109	7	2.26			
90	s	49	GE	51	9	2.00		120		h	53	G	63	1	2.02			
100	h	37	F	44	4	1.96		150		h	58	GE	148	20	2.37			
110	h	44	F	46	3	2.01		180		h	62	FG	58	7	2.14			
120	s	42	GE	27	4	1.69		85		30	h	60	FG	41	8	1.97		
130	h	51	FP	25	2	1.95				90	h	57	FG	35	1	1.87		
140	h	42	FP	28	2	1.96				150	h	59	F	28	2	1.90		
150	h	46	F	42	2	1.98				-90	h	62	GE	49	2	1.93	
160	h	50	FP	24	3	1.93												
170	h	55	G	40	3	1.83												
180	h	60	G	43	4	1.91												

tually counted) and ΔZ , ΔQ , and ΔE as derived from Tables VI, VII, and IX, respectively. The first entry ($\beta = +90^\circ$), for instance, represents an hour's exposure with the 100-inch of excellent quality at $Z = 39^\circ$, on which 71 nebulae were counted. $\log N_1$ is 1.85, ΔZ is 0.05, ΔQ and ΔE are both zero, hence $\log N$, the sum of these quantities, is 1.90.

Tables IIa, b, and c give the extra-survey plates conforming to the

standard conditions and centered on co-ordinates, stars, or small planetaries. The arrangement is similar to that in Table I, with the addition of *E*, the exposure time in minutes. The 27 plates with twenty-minute exposures in Table II*c* were included as bearing on the relation between $\log N$ and $\log E$.

TABLE II*a**
100-INCH; EXTRA-SURVEY FIELDS

β	λ	<i>E</i>	<i>Q</i>	<i>Z</i>	N_1	<i>I</i>	$\log N$	β	λ	<i>E</i>	<i>Q</i>	<i>Z</i>	N_1	<i>I</i>	$\log N$
+85°	168°	60	GE	42°	130	6	2.21	-9°	42°	130	FG	38°	10	3	0.78
84	208	60	FG	46	64	6	2.07	9	119	60	G	10	5	1	0.80
81	231	60	FG	35	95	9	2.20	9	119	110	G	25	42	1	1.39
78	242	60	FG	23	54	5	1.92	12	78	60	FG	51	15	1	1.46
75	243	45	GE	24	43	3	1.86	14	133	100	FG	9	6	2	0.67
75	262	60	E	21	150	18	2.19	15	355	60	GE	46	9	1	1.07
74	249	60	F	21	83	5	2.21	16	10	60	G	41	27	3	1.59
74	262	60	E	23	120	13	2.09	16	158	50	G	28	12	2	1.31
74	276	60	E	28	127	27	2.12	21	90	60	FG	13	87	5	2.12
73	250	60	E	29	132	16	2.14	22	89	60	G	14	71	12	1.95
73	250	60	FG	30	68	2	2.04	22	90	60	G	6	92	13	2.06
73	288	60	E	25	138	8	2.16	25	139	50	FG	32	33	3	1.84
72	237	60	G	31	58	11	1.89	27	191	60	GE	56	65	7	1.99
72	300	60	GE	32	138	13	2.21	37	22	40	G	45	14	0	1.55
70	229	60	G	22	252	22	2.51	37	93	60	GE	37	62	9	1.87
70	253	60	G	43	71	4	2.01	40	145	60	GE	35	29	2	1.54
70	310	60	GE	28	106	30	2.35	40	155	60	G	48	36	4	1.75
67	221	60	G	27	84	4	2.04	42	104	30	E	15	42	6	2.02
66	255	60	FG	41	80	10	2.14	52	87	60	GE	28	41	1	1.67
65	323	60	GE	37	152	15	2.26	53	187	60	FG	60	48	7	2.04
63	0	150	GE	40	363	41	2.12	54	22	30	G	46	23	1	1.94
63	257	60	FG	36	100	16	2.22	56	100	30	F	28	24	2	2.08
59	259	60	G	37	101	9	2.14	60	107	40	FG	45	41	4	2.09
58	318	30	FG	18	20	2	1.89	71	37	85	G	50	123	13	2.00
56	200	60	F	23	96	10	2.27	-72	40	135	GE	51	301	36	2.15
40	325	60	GE	46	41	0	1.73								
40	335	60	E	39	44	3	1.69								
34	232	60	FG	52	45	4	1.94								
28	39	60	GE	19	93	11	2.02								
+11	191	60	FG	46	16	2	1.46								

* *E* = exposure time in minutes. Two fields at $\beta = +73^\circ$, $\lambda = 250^\circ$ overlap about 10 per cent; two at $\beta = -9^\circ$, $\lambda = 119^\circ$ overlap about 5 per cent; two, $\beta = +75^\circ$, $\lambda = 243^\circ$ and $\beta = +28^\circ$, $\lambda = 39^\circ$, are also included in Table II*b*.

Tables III*a* and *b* list plates conforming to the standard conditions but centered on selected nebulae. Reduction to the homogeneous system requires elimination of the central nebulae and correction for the areas they cover, the corrected counts being designated by N'_1 . For this purpose the products of the two diameters in minutes of arc, *ab*, are listed, from which, on the assumption that the images approximate ellipses, the fraction of the inner circles, *I*, can readily be estimated. Since very large nebulae are not included in

the table, N'_i differs but little from N_i , and, in general, $N'_i = N_i - 1$ within the uncertainty of the counts; but for deriving distance cor-

TABLE IIb
60-INCH; EXTRA-SURVEY FIELDS

β	λ	E	Q	Z	N_i	I	$\log N$	β	λ	E	Q	Z	N_i	I	$\log N$
+87°	28°	90	G	33°	64	8	1.87	+28	39	60	GE	18°	54	9	1.94
85	13	90	G	36	124	21	2.16	23	187	60	G	30	67	2	2.12
80	163	60	E	12	85	6	2.09	15	25	60	G	5	22	6	1.60
78	172	90	GE	9	100	26	2.03	+13	19	60	G	14	14	1	1.41
75	243	60	GE	21	79	11	2.11	-12	119	60	FG	47	26	1	1.83
70	161	60	G	10	49	7	1.95	13	118	60	FG	11	48	3	2.02
69	228	60	FG	26	60	5	2.14	19	19	60	G	31	9	0	1.24
67	220	60	GE	37	91	10	2.20	25	15	60	GE	42	24	4	1.64
61	209	60	G	45	45	1	1.98	25	35	60	GE	26	18	2	1.48
60	158	60	G	33	23	3	1.65	26	95	60	G	8	67	8	2.09
60	201	60	GE	49	36	11	1.85	35	145	60	E	27	13	2	1.29
58	114	100	GE	27	176	15	2.18	36	60	60	G	19	75	5	2.15
58	299	60	GE	40	39	5	1.84	49	38	60	E	51	46	7	1.92
55	224	60	GE	51	44	6	1.94	-51	101	60	FG	32	17	3	1.60
54	201	60	G	28	133	13	2.41								
44	1	60	G	51	32	8	1.87								
41	206	60	GE	35	77	20	2.13								
40	59	60	GE	37	21	3	1.56								
35	112	60	GE	39	56	10	2.00								
+30	180	45	FG	21	23	2	1.88								

TABLE IIc*

60-INCH; EXTRA-SURVEY FIELDS; 20-MINUTE EXPOSURES

β	λ	Z	Q	N_i	I	$\log N_2$	β	λ	Z	Q	N_i	I	$\log N_2$
+75°	320°	32°	E	18	4	1.45	-45	109	33°	E	17	1	1.42
74	315	28	GE	10	0	1.22	53	52	32	E	19	1	1.47
73	313	25	E	18	2	1.44	54	36	42	GE	11	0	1.30
63	323	24	GE	24	2	1.60	54	51	34	E	13	1	1.31
63	325	24	E	15	1	1.36	55	35	45	E	13	3	1.34
62	338	28	GE	23	5	1.58	55	50	37	E	26	4	1.61
62	340	33	E	16	3	1.39	63	99	36	E	20	1	1.50
60	20	31	E	10	2	1.19	63	118	41	E	22	3	1.56
59	24	30	E	21	4	1.51	64	100	36	E	33	4	1.72
59	28	37	E	21	6	1.52	64	119	41	E	18	3	1.48
58	34	42	GE	6	1	1.04	65	100	38	E	34	4	1.74
58	36	31	GE	13	0	1.34	-65	120	40	E	21	3	1.53
58	40	38	GE	5	1	0.95							
53	294	42	GE	17	0	1.49							
+51	247	43	GE	10	0	1.26							

* N_2 = corrected number of nebulae for a 20^m exposure. To obtain $\log N$, corresponding to the standard one-hour exposure, add $\Delta E = +0.63$.

rections or "coma factors," by which the counts are eventually reduced to uniform definition over the entire plates equal to that in the central circles, the procedure is essential.

TABLE IIIa*
100-INCH; FIELDS CENTERED ON NEBULAE

NGC	β	λ	<i>E</i>	<i>Q</i>	<i>Z</i>	<i>N_c</i>	<i>I</i>	<i>ab</i>	<i>N'_i</i>	log <i>N</i>
4459.....	+87°	160°	60	GE	6°	66	5	60	71	1.89
4725.....	87	303	120	G	10	108	1	100	120	1.78
4008.....	79	169	60	FG	47	54	4	0.7	53	1.98
4293.....	79	230	60	G	29	72	14	27	76	2.00
			30	FP	39	12	2	27	11	1.94
4651.....	78	269	60	<i>F</i>	32	35	2	9	34	1.84
4192.....	75	240	40	<i>E</i>	25	77	1	100	84	2.17
4762.....	73	276	135	FG	29	157	21	8	156	1.92
4178.....	72	245	60	G	43	68	5	9.5	66	1.98
4124.....	71	242	60	GE	24	81	8	48	86	1.99
4535.....	70	261	60	<i>F</i>	31	53	1	100	56	2.06
4612.....	70	266	60	<i>F</i>	29	43	5	1.6	41	1.91
4532.....	68	262	60	FG	27	97	17	4.8	95	2.18
4215.....	67	250	40	G	37	40	6	0.3	39	1.96
3430.....	65	162	60	<i>F</i>	31	46	5	0.2	45	1.96
				•						
3489.....	63	203	60	G	26	75	8	2.1	74	1.99
5363.....	62	310	45	<i>E</i>	30	38	4	2.6	37	1.77
3412.....	60	202	45	<i>F</i>	35	20	1	2.5	19	1.77
5829.....	59	0	80	G	14	187	35	3.2	187	2.20
4593.....	57	268	60	G	39	78	5	12	78	2.04
3521.....	53	223	60	G	34	55	1	100	61	1.93
4742.....	52	272	90	<i>F</i>	46	38	6	37	1.70
5713.....	51	320	40	GE	47	50	8	4	49	2.04
2859.....	47	159	135	FG	20	146	11	19	147	1.89
2830.....	46	159	60	<i>E</i>	14	83	14	82	1.91
5850.....	46	329	110	G	45	140	15	19	142	1.97
5904.....	44	340	60	G	29	37	4	28	37	1.69
2712.....	43	144	45	FG	12	55	3	1.6	54	2.08
2693.....	42	135	20	<i>F</i>	20	10	2	0.3	9	1.87
5812.....	42	318	45	G	42	19	4	1	18	1.59
5990.....	41	337	60	G	32	35	7	1.4	34	1.66
6014.....	40	344	60	FG	32	47	4	0.8	46	1.87
2639.....	39	135	45	FG	22	28	8	0.3	27	1.79
6070.....	34	340	60	G	45	51	10	5.8	51	1.88
6080.....	34	342	60	GE	41	67	15	0.5	66	1.92
2545.....	28	169	60	GE	40	54	11	2.2	53	1.81
2855.....	27	212	45	<i>F</i>	50	20	1	2.3	19	1.83
6280.....	26	354	60	G	27	23	5	0.1	22	1.46
2642.....	23	198	60	<i>F</i>	51	13	1	13	12	1.46
6296.....	+23	352	60	GE	29	27	4	1	26	1.47

* *N'_i* is derived from *N_c* by rejecting the central nebula and correcting for the area which it covers. If the product of the two diameters, *ab* in the ninth column, is not listed, the nebula falls outside the central circle, *I*, and, while the nebula is omitted in deriving *N_c*, the correction for the area covered is negligible. The four cases for which *ab*=100 refer to central nebulae so large that the entire central circles are omitted.

Duplicate plates are included for NGC 4293 and 524.

The two nebulae, $\beta = -47^\circ, \lambda = 61^\circ$, and $\beta = -51^\circ, \lambda = 54^\circ$, are uncatalogued.

Plates in the Virgo cluster with the numbers of nebulae omitted in the reductions as presumably members of the cluster are:

NGC 4293.....	1 neb.	NGC 4124.....	2 neb.
4651.....	1	4535.....	3
4192.....	2	4612.....	2
4762.....	3	4532.....	3
4178.....	2	4215.....	1

The following fields are in both Tables IIIa and IIIb:

FIELD	LOG <i>N</i>	
	60-In.	100-In.
NGC 4762.....	1.87	1.92
4535.....	2.06	2.06
2859.....	2.03	1.89
4454.....	2.03	1.93

TABLE IIIa—Continued

NGC	β	λ	E	Q	Z	N_1	I	ab	N'_I	$\log N$
6384.....	+20°	358°	50	FG	20°	13	2	14	12	1.39
6610.....	13	10	60	G	20	14	2	0.1	13	1.22
6661.....	13	10	60	G	16	33	6	1.5	32	1.62
6674.....	13	22	70	FG	10	11	1	6.7	10	1.09
6710.....	+11	25	60	FG	21	20	3	1	19	1.47
6921.....	- 9	35	75	G	17	10	5	0.2	9	0.93
2325.....	10	208	45	F	63	7	3	0.3	6	1.44
147.....	14	87	90	GE	23	38	8	32	40	1.42
185.....	14	89	75	G	14	33	8	12	33	1.49
IC 5180.....	15	60	60	GE	13	53	9	1.1	52	1.76
6814.....	17	357	60	G	45	6	1	6.7	5	0.87
IC 5000.....	18	18	60	FG	37	24	3	23	1.58
6906.....	19	18	60	FG	31	13	4	2.1	12	1.29
6928.....	19	22	60	GE	24	50	11	2	49	1.75
6944.....	21	20	60	FG	27	25	4	0.1	24	1.58
7363.....	22	63	40	GE	24	49	6	0.8	48	1.97
6909.....	23	22	60	FG	33	18	2	0.5	17	1.44
7033.....	23	32	60	G	20	51	14	0.1	50	1.81
6915.....	24	9	75	GE	44	56	8	0.5	55	1.72
6954.....	24	18	60	G	37	9	4	0.4	8	1.04
6062.....	27	15	60	FG	34	40	6	6.5	39	1.81
7040.....	27	27	60	G	27	21	4	0.6	20	1.42
1156.....	28	125	45	FG	10	39	2	7.5	38	1.93
7177.....	30	43	90	G	35	82	9	6.3	82	1.82
7046.....	31	22	60	E	35	95	9	94	2.01
IC 1380.....	34	24	60	GE	42	63	13	62	1.80
7102.....	34	30	60	FG	32	44	10	2.2	43	1.84
1507.....	35	161	60	E	37	49	6	2.8	48	1.72
160.....	39	87	60	E	31	215	18	4	215	2.36
169.....	39	87	75	E	11	76	5	0.4	75	1.75
7454.....	40	57	120	G	34	157	16	0.4	156	1.93
1453.....	41	161	80	FP	47	36	4	0.6	35	1.90
877.....	43	121	60	E	19	61	8	60	1.79
.....	47	61	40	E	23	31	6	0.2	30	1.72
.....	51	54	30	E	29	22	3	0.1	21	1.74
524.....	52	106	60	GE	41	54	6	4.4	53	1.82
.....	150	FG	28	134	17	4.4	134	1.80
741.....	53	120	60	G	32	96	13	0.6	95	2.11
7393.....	55	34	110	GE	41	132	12	2.2	131	1.87
7785.....	55	66	60	FG	40	51	7	1	50	1.93
718.....	55	118	60	E	30	76	6	5.7	75	1.91
1084.....	55	151	60	G	43	44	5	6.7	43	1.79
488.....	56	106	90	FG	30	134	15	18	136	2.11
1042.....	56	151	60	GE	43	55	7	16	55	1.84
7716.....	58	57	60	FG	34	62	5	4.3	61	2.01
200.....	59	87	60	E	44	200	16	2.6	199	2.37
521.....	60	111	60	FG	42	109	6	9	108	2.27
533.....	60	111	45	E	33	135	15	134	2.33
IC 48.....	70	89	90	G	43	142	12	1	141	2.08
210.....	76	85	60	GE	50	82	6	21	82	2.05
578.....	78	157	90	G	58	120	10	10	120	2.11
134.....	83	296	60	FG	69	23	3	8.7	22	1.84
289.....	-85	245	60	G	66	67	2	40	67	2.19

TABLE IIIb*

60-INCH; FIELDS CENTERED ON NEBULAE

NGC	β	λ	E	Q	Z	N_1	I	ab	N'_1	$\log N$
4251.....	+84°	165°	60	GE	24°	93	10	1.8	92	2.18
4203.....	82	139	50	G	4	41	8	6.6	40	1.97
5127.....	81	28	50	G	33	38	4	0.6	37	1.97
4450.....	80	249	45	E	25	57	5	10	54	2.08
3900.....	77	180	60	GE	34	58	8	2.4	57	2.00
4421.....	77	250	50	G	44	20	1	1	17	1.67
3041.....	76	138	45	G	24	33	6	2.8	32	1.96
4267.....	75	247	45	F	28	49	7	5.5	45	2.28
4377.....	75	250	50	GE	30	61	13	1	57	2.10
4406.....	75	251	60	GE	40	80	9	5.5	70	2.10
4552.....	75	261	80	G	22	55	8	2.6	50	1.80
3813.....	74	144	60	FP	15	31	1	2.1	30	2.09
4138.....	73	110	50	G	34	37	4	1.3	36	1.97
4111.....	73	113	50	FG	11	86	13	4	85	2.38
4452.....	73	253	60	GE	23	119	15	0.5	116	2.27
4596.....	73	266	40	G	54	17	1	3.2	15	1.79
4762.....	73	276	60	FG	39	32	7	8	30	1.87
4451.....	71	257	50	GE	35	50	8	0.4	46	2.01
4098.....	71	272	40	G	38	24	3	3.8	23	1.90
5297.....	70	57	50	G	12	44	5	8	43	2.00
4535.....	70	261	40	G	40	36	3	36	33	2.06
3949.....	68	113	40	GE	37	19	7	3.1	18	1.73
3655.....	68	206	50	G	39	43	6	1	42	2.04
3803.....	67	113	50	G	36	41	8	12.3	41	2.02
3877.....	67	115	60	FG	19	46	3	3.1	45	2.00
3605.....	67	198	60	G	27	46	6	45	1.93
3607.....	67	198	90	G	34	59	6	1.5	58	1.83
4586.....	67	266	60	G	35	46	4	4.1	44	1.94
4157.....	66	104	60	GE	17	53	5	7.2	52	1.93
4088.....	65	105	45	F	30	24	3	9.5	23	2.00
3953.....	65	108	60	G	37	53	5	15	52	2.02
3432.....	65	154	50	FG	46	41	4	0.2	40	2.13
3628.....	65	210	60	E	24	85	7	2	84	2.10
5250.....	64	71	50	FG	47	23	3	0.2	22	1.87
4102.....	64	103	60	G	24	82	7	5.4	81	2.19
3414.....	64	170	60	GE	37	74	7	73	2.10
3437.....	64	185	60	G	17	63	7	1.8	62	2.06
4179.....	63	253	35	FG	57	8	1	1.1	6	1.58
5772.....	61	35	60	GE	31	46	9	2	45	1.88
5689.....	60	52	80	FP	49	20	2	1	19	1.81
3631.....	60	115	70	FG	29	56	7	16	56	2.02
5473.....	59	66	45	G	35	33	5	1	32	1.98
5485.....	59	66	45	G	30	51	8	1	50	2.16
4814.....	59	87	60	G	26	67	9	66	2.10
4500.....	59	93	50	G	24	40	7	2.3	39	1.98
5204.....	58	80	45	GE	33	33	6	10.4	32	1.91
3549.....	58	117	50	FG	41	24	3	3	23	1.87
5585.....	57	65	40	GE	38	39	5	24	39	2.07
3945.....	57	101	45	FG	29	30	2	2.1	29	1.99
3895.....	+57	103	50	E	26	46	7	0.8	45	1.94

* Plates in the Virgo cluster with the numbers of nebulae omitted in the reductions as presumably members of the cluster are:

NGC 4450.....	3 neb.	NGC 4596.....	2 neb.
4421.....	3	4762.....	3
4267.....	4	4451.....	4
4377.....	4	4098.....	1
4406.....	10	4535.....	3
4552.....	5	4586.....	2
4452.....	3	4179.....	2

TABLE IIIb—Continued

NGC	β	λ	E	Q	Z	N_1	I	ab	N'_I	$\log N$
5576.....	+57°	317°	40	FG	38°	26	5	0.8	25	2.02
5631.....	56	65	60	GE	31	74	6	1	73	2.09
5379.....	56	74	40	GE	36	25	2	24	1.85
3642.....	56	108	60	G	29	81	9	17.5	81	2.10
3610.....	56	110	45	GE	25	50	7	1	49	2.08
3189.....	56	180	45	E	12	36	5	3.6	35	1.87
5322.....	55	76	90	G	36	78	8	2	77	1.96
3488.....	55	114	50	F	38	58	8	1.8	57	2.36
3458.....	55	115	120	FG	31	92	3	3	91	1.03
4995.....	55	281	40	G	57	26	6	0.3	25	2.04
5820.....	54	56	60	GE	24	71	20	0.3	70	2.07
5216.....	54	81	45	FG	33	46	5	0.3	45	2.19
4609.....	54	272	50	G	42	51	7	8.5	50	2.13
4958.....	54	280	50	G	43	66	9	4	65	2.24
4125.....	52	96	45	FG	36	18	5	2	17	1.78
3021.....	52	160	50	F	39	32	2	1.5	31	2.09
3206.....	51	121	45	E	19	41	6	5.6	40	1.94
2971.....	51	155	60	F	15	36	4	0.6	35	1.98
3182.....	50	119	45	E	29	33	6	0.5	32	1.86
3682.....	49	102	60	GE	34	62	13	0.7	61	2.03
4250.....	47	93	60	FP	35	11	1	3	10	1.65
2859.....	47	159	45	E	27	49	5	12	48	2.03
5846.....	47	328	60	GE	40	45	8	1	44	1.89
2950.....	46	122	45	GE	38	32	4	1.1	31	1.91
5984.....	46	351	60	GE	32	58	6	2.2	57	1.99
2841.....	45	135	80	G	24	87	5	36	87	2.05
2782.....	45	150	45	FP	21	20	2	3.6	19	2.07
5044.....	45	280	40	GE	55	50	7	0.5	49	2.25
5970.....	45	346	45	GE	27	61	11	4.3	60	2.17
2770.....	44	159	60	FG	20	46	7	4.4	45	2.00
3516.....	43	100	60	FG	42	43	5	1.6	42	2.02
6143.....	42	52	60	GE	26	57	12	0.8	56	1.97
5832.....	42	76	45	GE	45	24	2	5	23	1.80
3348.....	42	102	50	E	41	49	7	0.6	48	2.01
3034.....	42	108	90	F	37	29	2	40	28	1.70
2742.....	41	122	45	G	26	13	2	4.8	12	1.53
3147.....	40	103	45	F	40	11	3	3.6	10	1.66
2787.....	39	111	45	F	41	22	5	2.8	21	1.99
3003.....	38	347	60	G	34	26	3	2	25	1.70
2608.....	37	162	40	FG	36	16	2	2	15	1.79
2650.....	36	111	45	E	42	36	6	1.2	35	1.93
2974.....	36	208	45	G	44	34	10	0.4	33	2.02
2748.....	35	103	45	GE	23	16	1	0.8	15	1.56
2633.....	35	106	60	G	48	41	4	4.9	40	1.95
2775.....	35	193	50	G	40	79	7	9	78	2.31
6359.....	34	58	35	G	30	9	3	1	8	1.50
6217.....	34	78	30	F	44	12	3	3.8	11	1.95
2732.....	34	100	45	G	46	30	6	0.5	29	1.97
2715.....	34	102	45	F	44	12	2	6.8	11	1.72
2655.....	33	102	60	FG	48	32	6	30	32	1.94
2543.....	33	153	45	G	33	44	5	43	2.09
6690.....	27	68	60	FG	43	49	4	48	2.08
2424.....	27	149	60	F	20	29	3	2	28	1.90
6240.....	26	348	60	GE	38	23	9	1.4	22	1.79
2781.....	24	212	50	FG	53	27	2	1	26	1.98
2380.....	23	153	60	FG	15	45	7	3.4	44	1.98
2811.....	23	215	60	G	50	15	1	1.2	14	1.51
6732.....	20	50	60	FP	19	17	7	1	16	1.82
1530.....	18	103	90	FG	42	17	1	20	16	1.37
6824.....	+15	55	60	GE	22	24	10	1.2	23	1.57

On plates in the Virgo cluster all nebulae brighter than about the fifteenth magnitude have been omitted as presumably members of the cluster—perhaps an unnecessary refinement, but consistent with the general principle of omitting the great isolated clusters in discussing the general distribution of the background on which they

TABLE IIIb—Continued

NGC	β	λ	E	Q	Z	N_1	I	ab	N'_I	$\log N$
6570.....	+14°	9°	60	G	21°	12	4	1.4	11	1.31
6615.....	12	9	60	G	27	9	2	0.3	8	1.18
IC 1303.....	+ 7	37	55	FG	16	19	2	1	18	1.66
1233.....	-15	119	60	FP	5	7	1	1.5	6	1.39
1003.....	17	112	60	G	22	55	10	5.3	54	2.00
7640.....	19	73	45	G	20	24	8	23	1.80
IC 1320.....	21	15	60	GE	35	19	3	0.3	18	1.50
925.....	24	113	60	F	10	16	2	96	16	1.64
753†.....	25	105	60	G	10	35	4	7.8	34	1.79
			45	GE	15	45	5	7.8	44	2.00
1620.....	28	164	50	FP	35	21	5	2.4	20	2.06
1588.....	29	162	60	FG	33	38	6	37	1.94
IC 1377.....	32	25	60	GE	36	42	3	0.4	41	1.85
IC 1401.....	38	27	60	GE	33	29	5	1.6	28	1.68
7448.....	40	56	60	GE	27	56	4	55	1.96
7454.....	40	57	45	G	25	39	7	0.5	38	2.03
7374.....	42	49	60	E	24	54	11	0.4	53	1.90
7385.....	42	51	60	GE	28	120	23	0.3	119	2.30
IC 1437.....	44	33	50	G	43	24	5	0.5	23	1.79
7409.....	46	52	60	G	31	63	8	2.2	62	2.08
660.....	47	111	60	FG	28	60	9	31	61	2.15
IC 5241.....	48	40	60	GE	44	40	7	0.4	39	1.86
IC 1460.....	49	47	60	GE	33	63	9	0.1	62	2.02
7743.....	50	66	60	E	26	78	18	2.2	77	2.07
1073.....	50	139	60	G	34	45	4	20	44	1.94
7541.....	51	52	60	GE	31	35	4	3.3	34	1.76
95.....	52	81	60	GE	25	55	10	2.3	54	1.95
936.....	54	136	75	G	36	96	23	11.2	96	2.15
193.....	59	87	60	G	38	58	7	57	2.07
196.....	62	87	60	FG	38	77	12	0.6	76	2.27
779.....	62	132	100	F	41	73	10	4	72	2.07
596.....	-66	121	40	G	42	27	2	26	1.96

† A duplicate plate of NGC 753 is included which gives the maximum difference in $\log N$ derived from an examination of about forty pairs of duplicates. This difference of 0.21 corresponds to a difference in limiting magnitude of the order of 0.35, which must be accounted for by variations in sky transparency, emulsion, definition, and development.

are spotted. The list of omissions, given in footnotes to Tables IIIa and b, indicates their small or negligible effect on the general statistical results.

Table IVa gives 139 extra-survey plates on which no nebulae were found. These, together with 75 such fields in the survey, determine the zone of avoidance. Table IVb lists 28 plates bordering the zone of avoidance, on which a few nebulae were found. These plates do

not conform to the survey conditions but are useful in defining the borders of the zone. Positions alone are listed in Tables IV, but in all cases the exposures are equivalent to at least an hour on fast plates with the 60-inch reflector.

TABLE IVa
FIELDS WITH NO NEBULAE

β	λ	β	λ	β	λ	β	λ	β	λ
+35°	334°	+ 6°	330°	+ 2°	336°	- 1°	319°	- 4°	355°
20	75	5	21	+ 1	28		345	5	4
20	85		34		20	2	35		28
20	323		35		36		53	6	14
18	350		61		55		56		62
16	321		199		159		334		91
15	346		347		179		335		353
14	71		349		195	2	343	7	133
	320	4	22		30	2	346	8	22
	321		35	0	34		348		356
	344		106		37		349	9	164
13	337		124		46		354	10	181
12	0		156		73		355		182
	74		162		78	3	26	12	142
	330		350		80		198	13	173
	340	3	8		110		199	14	136
	350		45		188		333		137
10	73	3	46		317		334	15	174
	335	3	87		321		339		175
9	6		106		335		353	17	128
	68		171	- 1	1		354	18	176
8	10	+ 2	43		27	- 4	10	19	125
	333		48		52		37		126
7	112		105		54		152	20	126
	329		142		91		205		144
	330		169		140		330	21	126
+ 6	14		170		193		335	-23	171
	65		171		205		336		

TABLE IVb
SUPPLEMENTARY LIST OF FIELDS WITH VERY FEW NEBULAE

β	λ		β	λ		β	λ	
+30°	335°	Field	+12°	108°	IC 342	-10°	99°	Field
25	325	Field	11	20	Field	12	43	NGC 7013
20	65	Field		63	NGC 6946	13	52	IC 1392
19	309	NGC 5968		213	2613	16	0	NGC 6821
18	321	6093	10	312	IC 4597		172	IC 423
14	106	IC 356	+ 9	333	NGC 6333	22	134	Pleiades
	165	NGC 2339	- 7	161	Field	25	355	Field
13	0	6509	9	34	Field	-35	135	Field
+12	11	6627		40	Field			
	55	Field	-10	43	Field			

The complete data, including about 1283 independent samples covering a total area of about 650 square degrees, or a trifle more than 2 per cent of the three-quarters of the sky included in the survey, are summarized in Table V. They comprise fairly comparable

groups representing the two telescopes and the survey and extra-survey fields. The groups for the two hemispheres are roughly in

TABLE V
SUMMARY OF OBSERVATIONAL DATA

	100-INCH		60-INCH		TOTAL	
	Fields	Neb.	Fields	Neb.	Fields	Neb.
Survey, Table I.....	387	13,130	378	11,515	765	24,645
Extra-survey, Tables II.....	55	4,412	61	2,331	116	6,743
Extra-survey, Tables III.....	93	5,685	142	6,128	235	11,813
Total.....	535	23,227	581	19,974	1,116	43,201

Extra-survey blank fields, Table IVa 139

Supplementary, Table IVb 28

Total fields 1,283

Polar Caps

	NORTH		SOUTH		TOTAL	
	Fields	Neb.	Fields	Neb.	Fields	Neb.
Survey.....	247	10,693	150	6,461	397	17,154
Extra-survey.....	179	10,666	65	4,363	244	15,029
Total.....	426	21,359	215	10,824	641	32,183

Galactic Belt

	Fields	Neb.	Fields	Neb.	Fields	Neb.
Survey.....	207	4,409	161	3,082	368	7,491
Extra-survey.....	129	1,459	145	2,068	274	3,527
Total.....	336	5,868	306	5,150	642	11,018

proportion to the relative areas over which they are distributed. The various groups have been analyzed separately and collectively, but

the only striking differences are the systematically larger values of $\log N$ for the extra-survey plates in high latitudes as compared with those for the survey. The excess amounts to approximately 0.10 in $\log N$ or about 25 per cent in the numbers. Various possible explanations were considered, but eventually the two groups were simply combined for evaluating the final results. The discussion, however, should be followed with this discrepancy in mind.

REDUCTION TO A HOMOGENEOUS SYSTEM

The data were reduced to a homogeneous system by applying the corrections ΔZ , ΔQ , and ΔE as already mentioned, and thus corrected were used to investigate the distribution over the sphere to a uniform but undetermined limiting magnitude. The results are independent of the second part of the investigation, in which the data are reduced to numbers of nebulae per unit area to definite limiting magnitudes. The final reductions are the culmination of a series of successive approximations of which only the later stages will be presented in detail. Preliminary analysis led to the following general conclusions, which are merely more precise formulations of previous indications:¹⁶

1. No nebulae are found along the heart of the Milky Way. The zone of avoidance is irregular and unsymmetrical, the width varying from 10° to 40° .

2. Nebulae are scarce along the borders of the zone and in certain regions the scarcity can be followed out to latitude 40° .

3. In the higher latitudes the nebular distribution, to a first rough approximation, is random, with occasional clusters superposed.

4. In the higher latitudes the numbers of nebulae increase with limiting magnitudes (or exposure times) at a rate which indicates a fair approximation to uniform distribution in depth, i.e., $\log N_m = 0.6m + C$.

On the basis of these results, the sphere was divided into the galactic belt ($\beta = -40^\circ$ to $+40^\circ$) and the polar caps ($\beta = 40^\circ$ to 90°). Data in the polar caps were assumed to represent nebular distribution alone; those in the galactic belt, a combination of nebular distribution and local galactic obscuration. Since the preliminary results in-

¹⁶ *Publications of the Astronomical Society of the Pacific*, 43, 282, 1931.

licated an approximately uniform or random distribution in the polar caps, the corrections ΔQ and ΔE , for quality of images and exposure times, were derived from those regions alone.

ATMOSPHERIC EXTINCTION

As a first step the counts were corrected for atmospheric extinction by adding to $\log N_i$ or $\log N'_i$ the factor

$$\Delta Z = 0.6 \Delta m,$$

where Δm is the extinction in photographic magnitudes at zenith distance Z , taken from the table in current use at Mount Wilson.¹⁷ The coefficient 0.6 follows from No. 4 of the preliminary results. Since the relation

$$\log N_m = 0.6m + C$$

holds approximately over a considerable range in m , the assumption that it holds precisely over the limited range in atmospheric extinction covered by the observations will not introduce serious errors.

The corrections are listed in Table VI as a function of Z . Up to $Z = 60^\circ$ the values were interpolated from a smooth curve constructed from the extinction tables. Beyond 60° they are extrapolations following the theoretical trend of extinction-curves; but since very few plates were exposed at low altitudes, the uncertainties are not important. The values of ΔZ in Tables I–III range up to 0.32, but only 18 exceed 0.20 and the mean is about 0.053.

The corrections might be applied to exposures rather than to the counts, thus avoiding the assumption of uniform distribution. This procedure, however, would introduce an assumption concerning the relation between limiting magnitude and exposure time which is probably as uncertain as that concerning distribution, and hence offers little advantage over the convenient method actually adopted.

CORRECTION FOR QUALITY OF IMAGES

The quality factor, ΔQ , is perhaps the most important and at the same time the most arbitrary factor in the entire investigation.

¹⁷ F. H. Seares *et al.*, *Carnegie Institution of Washington Publication*, No. 402; *Papers of the Mount Wilson Observatory*, 4, Introd., p. 36, 1930.

It measures the effect of definition on the threshold of identification or the ability to distinguish between nebulae and stars. The plates were rated on an arbitrary scale as "Excellent," "Good," "Fair," and "Poor," with the intermediate steps "GE," "FG," and "FP," according to the sharpness of the star images. For one-hour exposures in the polar caps, mean values of $\log N_r + \Delta Z$ were then derived

TABLE VI
CORRECTIONS TO $\log N$ DEPENDING ON ZENITH DISTANCE

Z	Δm_{pg}	ΔZ^*	Z	Δm_{pg}	ΔZ^*	Z	Δm_{pg}	ΔZ^*
10°	0.004	0.00	43°	0.06	57°	0.15
1601	4407	5816
20	.019	.01	45	0.122	.07	5917
2301	4608	60	0.295	.18
2402	4708	61	(.19)
2902	4809	62	(.20)
30	.046	.03	4909	63	(.21)
3303	50	.164	.10	64	(.23)
3404	5110	65	(.40)	(.24)
35	.065	.04	5211	66	(.26)
3704	5312	69	(.32)
3805	5412	70	(0.59)	(0.35)
40	0.090	.05	55	0.219	.13			
41	0.06	56	0.14			

* $\Delta Z = 0.6 \Delta m_{pg}$.

for each quality class.¹⁸ These values are listed in Table VII for each telescope and for survey and extra-survey groups, both separately and combined, together with the number of plates, n , and the mean latitude corresponding to each value. The latitudes are included because a correlation was found later between $\log N$ and β which, although of little importance in the higher latitudes, might possibly influence the derivation of the quality factors. Rereducations which take into account the latitude effect indicate, however, no very significant revisions of the factors actually adopted.

The data are presented graphically in Figure 1, where values of $\log N$ are plotted against quality classes, both for the survey alone and for the totals. The quality classes are arbitrarily separated by

¹⁸ Four fields were omitted as obviously affected by local obscuration. These are $\beta = +40$, $\lambda = 330^\circ$ and 340° ; $\lambda = 140^\circ$, $\beta = -40^\circ$ and -45° . One field ($\beta = +55^\circ$, $\lambda = 10^\circ$) was omitted because it includes a conspicuous cluster.

equal intervals along the horizontal axis. The curves for the two telescopes are approximately parallel, with a displacement of the

TABLE VII
QUALITY FACTORS

Q	SURVEY			EXTRA-SURVEY			TOTAL		
	n	log N	β	n	log N	β	n	log N	β
100-Inch									
E.....	17	1.838	66.2	9	2.076	63.6	26	1.920	65.3
GE.....	32	1.877	61.1	12	1.923	63.9	44	1.890	61.8
G.....	34	1.775	60.0	16	1.883	61.3	50	1.809	60.4
FG.....	38	1.720	57.0	14	1.870	67.2	52	1.761	59.7
F.....	35	1.633	55.3	6	1.761	68.8	41	1.652	57.3
FP.....	15	1.447	53.7	15	1.447	53.7
Total.....	171	1.730	58.6	57	1.906	64.2	228	1.774	60.1
60-Inch									
E.....	39	1.758	58.2	5	1.856	57.2	44	1.770	58.1
GE.....	56	1.696	54.1	26	1.799	56.6	82	1.729	55.1
G.....	33	1.627	56.5	15	1.765	59.1	48	1.670	57.3
FG.....	15	1.544	54.7	8	1.667	59.0	23	1.587	55.5
F.....	13	1.438	55.0	1	1.540	51.0	14	1.446	54.7
FP.....	1	1.340	40.0	2	1.260	60.5	3	1.287	53.7
Total.....	157	1.659	55.7	57	1.753	57.4	214	1.680	56.1
Q	100-INCH		60-INCH		MEAN LOG N	ΔQ	ADOPTED ΔQ		
	n	log N	n	log N + 0.16			100- Inch	60-Inch	
E.....	26	1.920	44	1.930	1.926	0.000	0.00	0.16	
GE.....	44	1.890	82	1.889	1.889	.037	.04	.20	
G.....	50	1.809	48	1.830	1.820	.106	.10	.26	
FG.....	52	1.761	23	1.747	1.756	.170	.18	.34	
F.....	41	1.652	14	1.606	1.640	.286	.28	.44	
FP.....	15	1.447	3	1.447	1.447	0.479	0.45*	0.61	

* The value 0.45 is adopted on the basis of results from 18 rejected FP plates.

order of 0.16 in log N. This quantity was accordingly added to log N for the 60-inch, and mean values were then derived from the data

for the two telescopes combined. Figure 1 indicates the fairly satisfactory manner in which the data are represented by smooth curves adjusted to the mean values.

More detailed information is furnished in Table VII. The outstanding residual in the curve representing all data combined (upper curve in Fig. 1) is the 60-inch point for quality F, which depends upon only 14 plates. Of the two large residuals for the survey alone

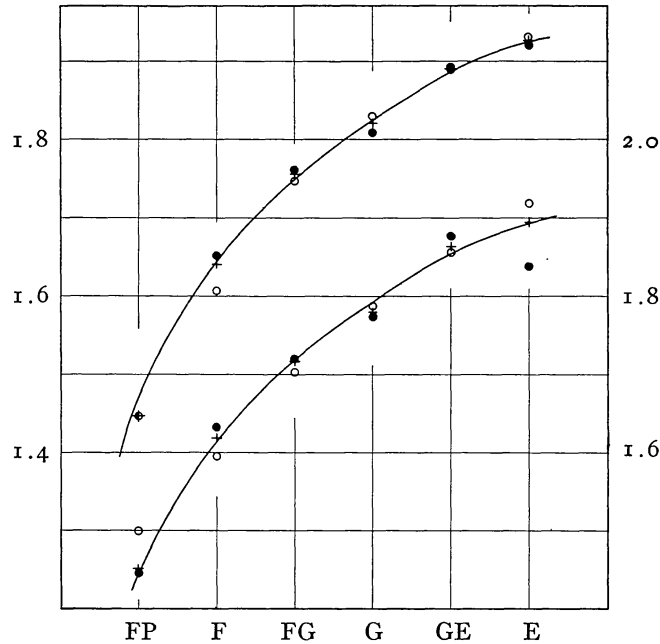


FIG. 1.—Quality factors. Mean $\log N$ for one-hour exposures, $\beta \approx 40^\circ$, plotted against quality classes. The lower curve represents the survey alone; the upper curve, all the data combined. Disks indicate data with the 100-inch; circles, with the 60-inch but with $\log N$ increased by 0.16; crosses, means for both telescopes, weighted according to the relative numbers of plates. Data from Table VII.

(lower curve) the 100-inch point for quality E depends upon 17 plates; the 60-inch point for FP on a single plate. Plates of quality P were in general discarded as unreliable, and the relatively few of quality FP that are included were retained for the sake of completeness when efforts at replacement had not succeeded. Examination of discarded plates suggested a slight revision of the quality factor for FP, indicated by the data in Table VII, and a tentative factor

of 0.70 for the two 100-inch P plates,¹⁹ which were retained for completeness. The adopted quality factors, ΔQ , listed at the end of Table VII, are slightly smoothed in order to represent a uniform progression, but, except for the FP factor already mentioned, the revisions do not exceed 0.01. The systematic term, 0.16, added to the factors for the 100-inch, gives factors for the 60-inch which reduce the counts to the standard conditions of excellent plates with the 100-inch.

The factors were derived from one-hour exposures alone and are assumed to apply over the entire range of exposures (20–150 min.). The data are too restricted for conclusive evidence on this point, but they are not inconsistent with the assumption. The quality scale is arbitrary, the smooth progression of the factors being more or less accidental. Each class covers a considerable range in the scale and this circumstance introduces an artificial scatter into the corrected counts. The procedure, in fact, represents a much-simplified statistical approximation, but it is doubtful whether the nature of the data justifies more refined methods.²⁰

CORRECTION FOR EXPOSURE TIME

Preliminary examination suggested that, as a first approximation, tripling the exposure quadruples the numbers of nebulae. Tripling the exposure was supposed to extend the limit by 1 mag. (the usual assumption in photographic photometry with fast plates); hence quadrupling the nebulae suggested uniform distribution in depth. The relation is

$$\begin{aligned}\log N &= \frac{0.602}{0.477} \log E + C, \\ &= 1.26 \log E + C.\end{aligned}$$

This relation ignores the effect of red shifts in diminishing apparent luminosities and assumes a deviation from the photographic reciprocity law represented by a value of about 0.84, for the Schwarzschild exponent p .

¹⁹ These are survey fields at $\beta = +35^\circ$, $\lambda = 300^\circ$ and $\beta = -15^\circ$, $\lambda = 140^\circ$. The data are uncertain but do not affect the general results.

²⁰ Since the number of FP plates is small, the greatest scatter should be in class F where, as indicated in Fig. 1, $\log N$ ranges from about 1.57 to 1.70. These plates were

Detailed analysis of the present data indicates, however, a coefficient for $\log E$ in the preceding relation definitely greater than 1.26; and interpretation of this result introduces problems of far wider significance than the immediate purpose, which is merely the reduction of the counts to a uniform exposure of one hour. Further discussion of these problems will be deferred, but it may be mentioned that the present results appear to represent the combination of a close approach to the reciprocity law²¹ under the particular observing conditions (small surface images at the threshold of Eastman 40 plates), which increases the coefficient, and the effect of the red shift, which diminishes the coefficient. This interpretation is sufficiently probable to justify the retention of the provisional assumption that the nebulae are distributed uniformly in depth.

In Figure 2, $\log N$ (representing the counts reduced to quality E with the 100-inch at the zenith) is plotted against $\log E$ (exposure time in minutes) for 636 fields in the polar caps (omitting the 5 fields not used in deriving the quality factors). A casual inspection indicates an approximately linear correlation in which the coefficient of $\log E$ is of the order of 1.3. The data are grouped according to a small number of values of $\log E$ and in each group of any considerable size the frequency distribution of $\log N$ approximates an error-curve more or less symmetrical about the mean value. The diagram is dominated by the excessively large group of one-hour exposures in which the range in $\log N$, as expected from the form of the frequency distribution, is disproportionately large. This restricts the significance of a correlation ratio and limits the analysis to the regression-curve of $\log N$ on $\log E$, or to the usual least-squares solution with the data grouped according to $\log E$. A direct solution

re-examined and divided into three groups, F+, F, and F-. $\log N$ then fell in the same order, but the results did not appear to justify the general application of the refinement.

²¹ Some observations bearing on the reciprocity law are mentioned later in connection with the determination of limiting magnitudes corresponding to particular exposure times. These data are more or less consistent with various recent investigations which tend to reduce the failure of the reciprocity law, at least for low intensities and fast plates, as compared with the results found in earlier investigations. See, for instance, Jones and Huse (*Journal of the Optical Society of America*, **11**, 338, 1925) for data on the fast Seed 30 plate and Twyman and Harvey (*Transactions of the Optical Society*, **33**, 1, 1931) for tests of the Schwarzschild relation at the threshold.

of this nature, with equal weights for all fields, leads to the relation

$$\log N = 1.290 \log E - 0.362, \quad (1)$$

which is indicated by a full line in the figure.

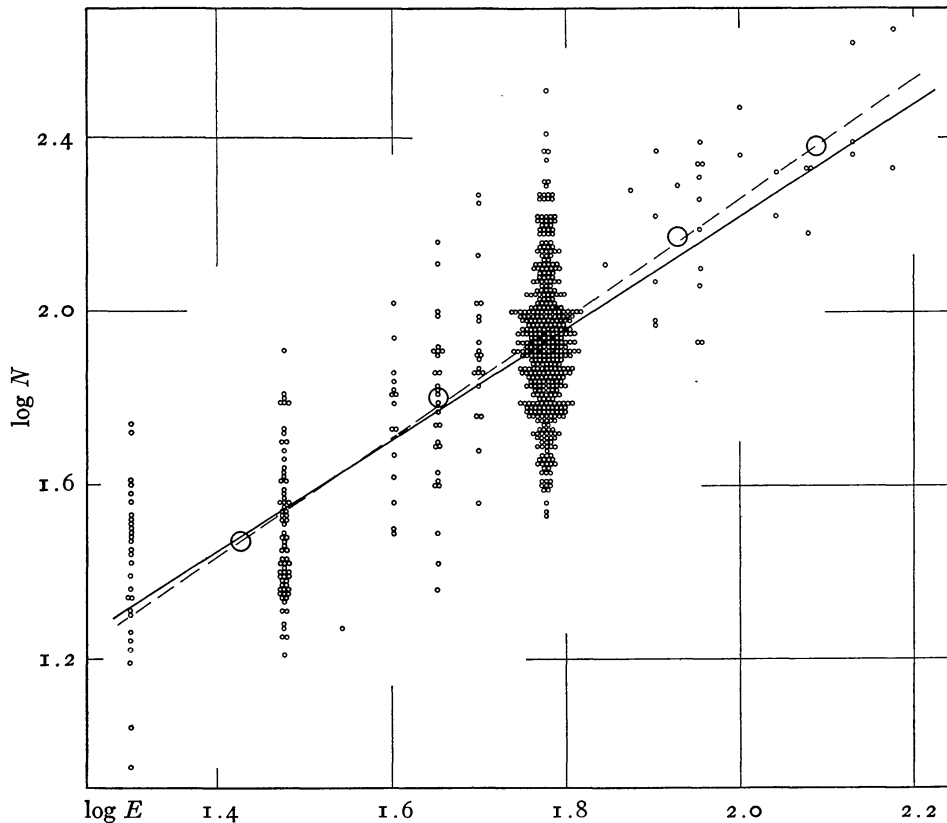


FIG. 2.—Log N as a function of exposure time. Log N , corrected for quality and atmospheric extinction, plotted against log E (exposure time in minutes) for all plates with $\beta \approx 40^\circ$. The five large circles are mean points from Table VIII, from which is derived the correlation indicated by the dash line ($\log N = 1.376 \log E - 0.493$). The full line is the relation, $\log N = 1.290 \log E - 0.362$, derived from a least-squares solution for a grouping according to log E with equal weights for all plates.

The assignment of equal weights, however, is open to criticism. If the nebulae are distributed approximately at random, the volume of space explored, and hence the number of nebulae recorded per plate, should increase with exposure and, of course, the errors of sampling should decrease as the size of the samples increases. The

weights, therefore, should increase with the exposure, and hence in Figure 2 the systematic departures of the longer exposures from the foregoing relation cannot be entirely ignored, notwithstanding the relatively small numbers of plates involved. The 30 plates with exposures longer than an hour represent about 5400 nebulae, as compared with about 6600 nebulae found on the 164 plates with exposures shorter than an hour. The relative weights of the two groups as derived from plates and from nebulae are about 1 to 5.5 and 1 to 1.2, respectively.

The effect of weighting according to numbers of nebulae can be partially ascertained by grouping the data for exposures other than one hour into mean points representing comparable numbers of nebulae and including the mean for the hour exposures with the same weight. The necessary data are found in Table VIII, which gives, both for plates centered on selected nebulae and for plates centered without reference to nebulae, the mean $\log N$ for each exposure time and for various groupings of the exposures. For the immediate purpose the significant data are the 3-groups and the 5-groups for all fields combined. These mean points lead to coefficients of $\log E$ equal to 1.364 and 1.376, respectively. The latter relation is indicated in Figure 2 by a dash line, and the 5-points from which it is derived are represented by large open circles.

Other methods of grouping the data lead to values of the coefficient of $\log E$ which, in general, lie between the extremes already mentioned, namely, 1.29 and 1.37. Largely for this reason, and without further discussion of the relative merits of weighting by plates or by counts, a value of 1.33 has been adopted for the reductions as a compromise. This arbitrary procedure is admittedly a makeshift to serve the immediate purpose. It has little justification beyond the fact that the corresponding corrections to $\log N$ differ from those derived from either extreme value by more than 0.01 only for the twenty-minute exposures and the four longest exposures for which the difference is 0.02. These quantities are well within the uncertainties of the counts. The corrections for each exposure time which reduce the values of $\log N$ to the standard exposure of one hour are given in Table IX.

APPARENT DISTRIBUTION OF NEBULAE

The general features of the apparent nebular distribution are indicated in Figure 3 where the fields are plotted by galactic co-ordinates on Aitoff's equal-area projection of the sphere. The term "nor-

TABLE VIII
RELATION BETWEEN LOG \bar{N} AND EXPOSURE TIME

EXPOSURE	SURVEY AND EXTRA-SURVEY FIELDS			FIELDS CENTERED ON NEBULAE		
	n	$\overline{\log N}$	$\overline{\log E}$	n	$\overline{\log N}$	$\overline{\log E}$
20 ^m	27	1.419	1.301	1	1.240	1.301
30.....	68	1.495	1.477	2	1.440	1.477
35.....				1	1.270	1.544
40.....	1	1.860	1.602	14	1.739	1.602
45.....	2	1.590	1.653	27	1.783	1.653
50.....				21	1.916	1.699
60.....	371	1.912	1.778	71	1.997	1.778
70.....				1	2.110	1.845
75.....				1	2.280	1.875
80.....				5	2.122	1.903
85.....	1	2.290	1.929			
90.....	3	2.250	1.954	7	2.157	1.954
100.....	1	2.470	2.000	1	2.360	2.000
110.....				2	2.270	2.041
120.....				3	2.280	2.079
135.....	1	2.620	2.130	2	2.375	2.130
150.....	1	2.650	2.176	1	2.330	2.176
Total....	476	1.830	1.711	160	1.942	1.754

3-Groups

20-50.....	98	1.480	1.435	66	1.789	1.646
60.....	371	1.912	1.778	71	1.997	1.778
70-150.....	7	2.397	2.014	23	2.214	1.986

ALL FIELDS

5-Groups				3-Groups			
20-30....	98	1.471	1.427	20-50....	164	1.604	1.518
35-50....	66	1.803	1.654	60....	442	1.925	1.778
60....	442	1.925	1.778	70-150....	30	2.257	1.992
70-90....	18	2.174	1.928				
100-150....	12	2.380	2.088				

mal distribution" is here applied to fields in which the numbers of nebulae lie between about one-half and twice the mean for fields within the polar caps; more precisely, $\log N = 1.63 - 2.22$. About 93 per cent of the fields in the polar caps fall within the definition and are unobtrusively represented by small dots. Excesses and deficiencies are indicated by black disks and open circles, respectively, and crosses are superposed where the deviations from the mean exceed 0.60 in $\log N$. Clusters, other than those appearing on survey plates, are omitted, and hence the crosses, with one exception,²² are confined

TABLE IX
CORRECTIONS WHICH REDUCE $\log N_1$ TO EXPOSURES OF ONE HOUR

E	ΔE^*	E	ΔE^*	E	ΔE^*
20 ^m	+0.63	60 ^m	0.00	100 ^m	-0.29
30	.40	70	-.09	110	.35
35	.31	75	.13	120	.40
40	.23	80	.17	130	.45
45	.17	85	.20	135	.47
50	+0.10	90	-0.23	150	-0.53

* $\Delta E = 1.33 \log E$.

to deficiencies referring to galactic obscuration. Fields with no nebulae are indicated by dashes and, with one exception,²³ fall within the zone of avoidance along the Milky Way. The large-scale features are as follows: An irregular zone of avoidance runs along the Milky Way and is bordered by partial obscuration which fades away into the general field of normal distribution. The influence of the Milky Way is most conspicuous in the direction of the center of the galactic system ($\lambda = 325^\circ \pm$), where it extends more than 30° on either side of the galactic plane. In the opposite direction ($\lambda = 145^\circ \pm$) there is extensive obscuration to the south (Taurus region), but on the northern side the normal distribution sweeps down to latitude 15° or less.

THE ZONE OF AVOIDANCE

The zone of avoidance was outlined from the distribution of dashes alone, although the inclusion of crossed circles might have

²² The cluster in Corona Borealis, falling in the survey field ($\beta = +55^\circ$, $\lambda = 10^\circ$).

²³ The small detached obscuring cloud near $\beta = +35^\circ$, $\lambda = 335^\circ$, marked *A*.

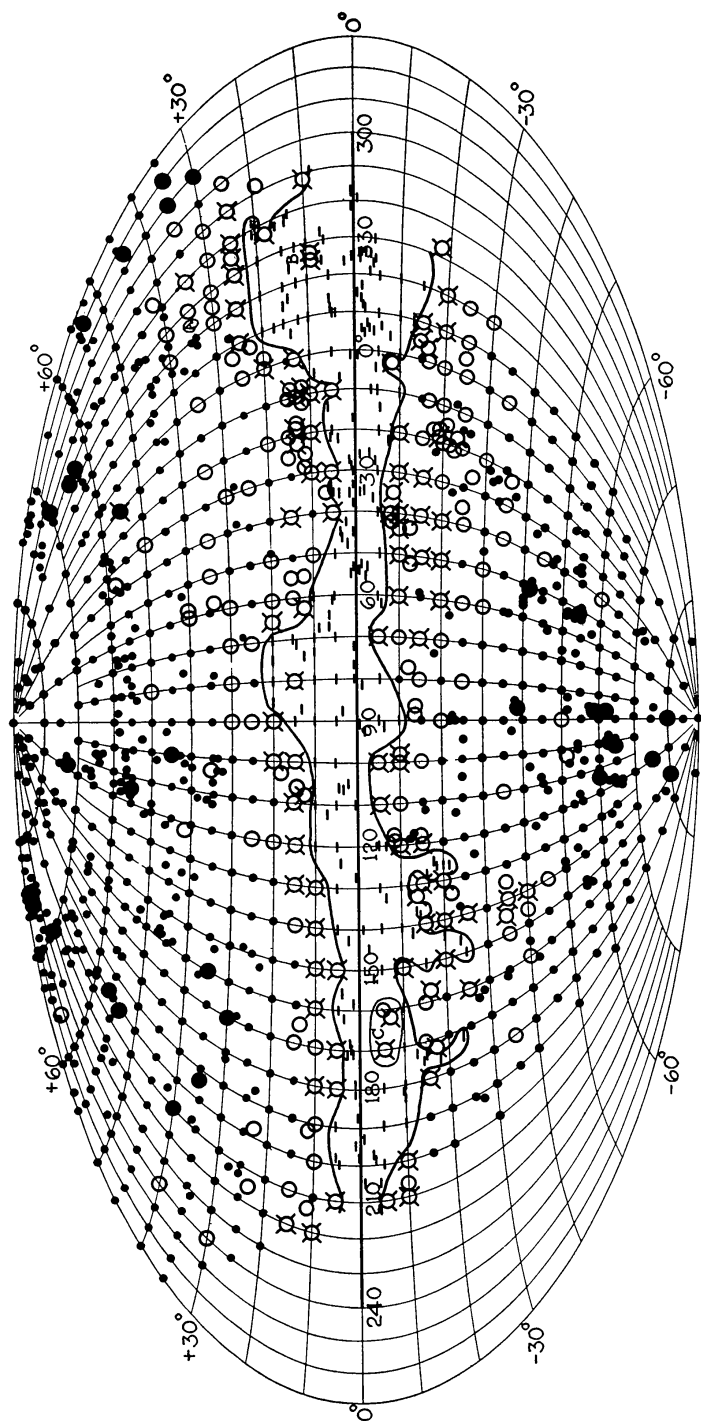


FIG. 3.—Distribution of extra-galactic nebulae. Small dots represent normal distribution ($\log N = 1.63-2.22$); large disks and circles represent excesses ($\log N = 2.23-2.52$) and deficiencies ($\log N = 1.33-1.62$); crosses are added where $\log N > 2.52$ or < 1.33 ; dashes represent fields with no nebulae.

enhanced its significance. Either method leads to the same general picture—a continuous irregular belt along the Milky Way with two small and significantly located exterior patches. The general pattern follows the distribution of known obscuring clouds, and the zone is presumed to represent analogous phenomena. The irregularity is strong evidence that the obscuration is due largely to isolated clouds rather than to a uniform layer of diffuse material.

The zone appears to consist of a narrow belt from 10° to 20° wide, centered approximately on the galactic plane, from which several great flares extend out into the higher latitudes. The two flares which extend to the highest latitudes coincide with the tips of the inclined belt of helium stars and diffuse nebulosity where it reaches its greatest departures from the galactic plane. These regions are the well-known areas in Ophiuchus and in Taurus, in the directions of the galactic center and anticenter respectively, the former representing the northern and the latter the southern reaches of the inclined belt. Beyond either tip are found the small detached outliers already mentioned²⁴—one patch of obscuration near $\lambda = 335^\circ$, $\beta = +35^\circ$, the other near $\lambda = 145^\circ$, $\beta = -35^\circ$. The regions covered by these flares are so well known from the many published reproductions of camera plates that further description is unnecessary. The narrow winding flare leading up to the Orion nebula may perhaps be regarded as a detached outlier from the Taurus flare.

The Cepheus flare, north of the galactic plane and between longitudes 60° and 100° , is perhaps less familiar, although camera plates indicate that the entire region is affected by considerable obscuration. The flare extends out to latitude 20° or more, and the partial obscuration along its borders includes the position of the celestial pole ($\lambda = 90^\circ$, $\beta = +28^\circ$). The partial obscuration accounts for the

²⁴ The northern field, marked *A* in Fig. 3, is in the vicinity of R.A. = $15^{\text{h}}46^{\text{m}} \pm$ Dec. $-3^\circ.5 \pm 1900$ (BD $-2^\circ.4064$ falls near the preceding edge of the north-following extension). It has long been known at Mount Wilson and parts were photographed with the 100-inch as early as 1923. The edge of the cloud is a striking object visually, and suggests the region south of ζ Orionis without the luminous background or the nebulous stars. The field was included by Lundmark and Melotte in their catalogue of dark markings found on the Franklin-Adams charts, but is about the only obscuring cloud catalogued in high latitudes whose nature is not questioned. The southern region, on the other hand, appears as an extensive area of partial obscuration with no conspicuous opaque clouds.

scarcity of nebulae in the immediate vicinity of the pole and probably affects some of the stars in the Polar Sequence. Fortunately, there is no reason to assume that the absorption is selective to any considerable degree, hence it may not seriously influence the relation between color index and spectral type as derived from the precise data of the sequence.

Within the zone as outlined by the dashes, five fields (two in the Ophiuchus flare marked *B*, two in the Taurus flare marked *C*, and one in the Cepheus flare) are included, in which occasional nebulae are recorded. Reference to camera plates indicates that these fields are relatively rich in stars and may represent thin spots in obscuring clouds. Those in Ophiuchus²⁵ are at $\beta = +9^\circ$, in the star clouds near the base of the dark lanes leading out to ρ Ophiuchi, and appear to be veiled by the flare rather than by the narrow belt along the galactic plane. At any rate, nebulae are consistently found at $\beta = +10^\circ$, some 35° away in longitude. It seems plausible to assume that the chances for thin spots are greater in the isolated flares than in the galactic belt where clouds may be scattered one behind the other to very great depths. The same supposition applies to the field in the Cepheus flare at $\beta = +15^\circ$ and perhaps to the Taurus flare as well, where, although the nebular fields are at $\beta = -5^\circ$, the galactic belt appears to be relatively narrow and where, moreover, the distribution of clouds in depth should be much less, since the direction is nearly opposite to that of the galactic center.

From $\lambda = 340^\circ$, where the survey begins, to about $\lambda = 70^\circ$ the southern hemisphere is affected by irregularly distributed partial obscuration reaching out in places to $\beta = -30^\circ$ and more, although the zone of avoidance, as arbitrarily defined, extends to less than 10° . The region might be described as a flare consisting of semi-transparent clouds. North of the galactic plane and in the same latitudes, i.e., between the Cepheus and the Ophiuchus flares, large open circles are mingled among dots in a manner which suggests isolated patches of obscuration in this region as well. Here also nebulae can be fol-

²⁵ Curtis found two nebulae in the field of NGC 6333, near this region, and also four in the adjacent Selected Area No. 133. Nebulae are found in both fields on the Mount Wilson plates, but others mentioned by Curtis in the zone of avoidance have not been confirmed.

lowed down close to the galactic plane. Three of the survey fields at $\beta = +5^\circ$ record nebulae, and a group of spirals (IC 1303, etc.) is found at $\beta = +7^\circ$.

REGION OF NORMAL DISTRIBUTION

Between the southern region of partial obscuration and the Taurus flare, the field of normal distribution sweeps up toward the galactic plane and reaches $\beta < 15^\circ$ in the vicinity of $\lambda = 110^\circ$. M 31, at $\beta = -22^\circ$, falls in this region, and also Wolf's cluster of nebulae in Perseus at $\beta = -12^\circ$. In the northern hemisphere, to the east of the Cepheus flare ($\lambda < 105^\circ$), the region of normal distribution again sweeps down to latitude 15° and is uninterrupted out to the limits of the survey, i.e., $\lambda = 210^\circ \pm$, where nebulae on opposite sides of the galactic plane are recorded only 10° apart. This latter region, just south of Sirius, represents the narrowest and least conspicuous portion of the Milky Way that falls within the survey.

The conspicuous effects of local obscuration are so extensive that they seriously limit the regions in which the real distribution of nebulae can be investigated with confidence. Irregular limits might be estimated from the manner in which the partial obscuration fades into normal distribution, but it seems less arbitrary to restrict the provisional investigation to the two polar caps. Analysis of the distribution in the polar caps leads to the following results:

1. There is no conspicuous systematic variation in longitude.
2. There is a definite variation in latitude closely approximating a cosecant law.
3. The frequency distribution of $\log N$ approximates a Gaussian error-curve.
4. The two caps, northern and southern, are similar, and the distributions agree within the uncertainties of the data.

DISTRIBUTION IN LONGITUDE

This feature was provisionally investigated along successive narrow zones of latitude in order to avoid the possibility of latitude effects, but no conspicuous harmonics were found. Similar investigations in the galactic belt, dodging the flares in the zone of avoidance, emphasized the contrast between the directions of the galactic

center ($\log N$ minimum) and the anticenter ($\log N$ maximum). Later, when the latitude effect was established and tentative cor-

TABLE X
LONGITUDE EFFECT IN $\log N$

λ	$\beta = 20^\circ - 30^\circ$				$\beta = 40^\circ - 50^\circ$			
	North		South		North		South	
	n	$\log N$	n	$\log N$	n	$\log N$	n	$\log N$
0°	2	1.885	2	1.790	4	2.080	3	2.033
10°	3	1.940	7	1.836	3	1.953	3	1.873
20°	3	1.867	5	1.774	3	2.010	3	2.150
30°	3	1.840	6	1.838	3	1.873	4	1.830
40°	4	1.992	3	1.817	3	1.907	5	1.896
50°	4	1.965	2	1.770	4	2.055	7	2.053
60°	2	1.890	3	1.883	4	1.765	7	1.981
70°	2	2.040	3	1.843	3	1.880	4	2.145
80°	1	1.890	3	2.037	4	1.807	3	1.900
90°	7	2.201	4	1.920	3	1.760
100°	2	1.895	5	2.164	7	1.839	4	1.972
110°	3	2.005	4	1.992	4	1.887	5	1.998
120°	3	1.797	4	2.040	6	1.897	4	1.900
130°	3	2.037	2	1.980	5	2.070	3	1.993
140°	3	2.087	2	2.130	4	1.970	4	1.887
150°	4	2.070	4	1.992	4	1.895
160°	3	2.023	4	2.052	7	2.016	4	1.965
170°	3	2.110	3	2.033	3	1.970	3	1.987
180°	4	2.035	3	1.937	3	1.910	3	1.983
190°	4	2.150	4	2.215	3	1.860	3	1.950
200°	4	1.975	2	2.110	3	1.920
210°	6	2.045	4	2.275
220°	3	2.113	3	1.997
230°	3	1.923	3	1.907
240°	2	1.915	3	1.833
250°	1	1.980	3	1.830
260°	3	1.813
270°	3	2.073
280°	4	1.945
290°	1	(2.410)*	3	2.033
300°	2	1.905	3	1.960
310°	3	1.827
320°	6	1.895
330°	6	1.882
340°	5	1.900
350°	3	1.820	1	1.830	5	2.022	3	1.900

* Quality FP, hence $\log N$ is uncertain and the corresponding point is omitted from Fig. 4.

rections could be applied, the distribution in longitude was re-examined on the basis of wider zones and the provisional results con-

firmed. The nature of the data and the results for two zones are indicated in Table X and in Figure 4. One zone, $\beta = 20^\circ$ to 30° , is in the galactic belt; the other, $\beta = 40^\circ$ to 50° , is the lowest zone in the polar caps.

Values of mean $\log N$ reduced to the galactic pole, together with the numbers of fields represented by the means, are tabulated for intervals of 10° in longitude. Omissions in the zone $\beta = 20^\circ$ to 30°

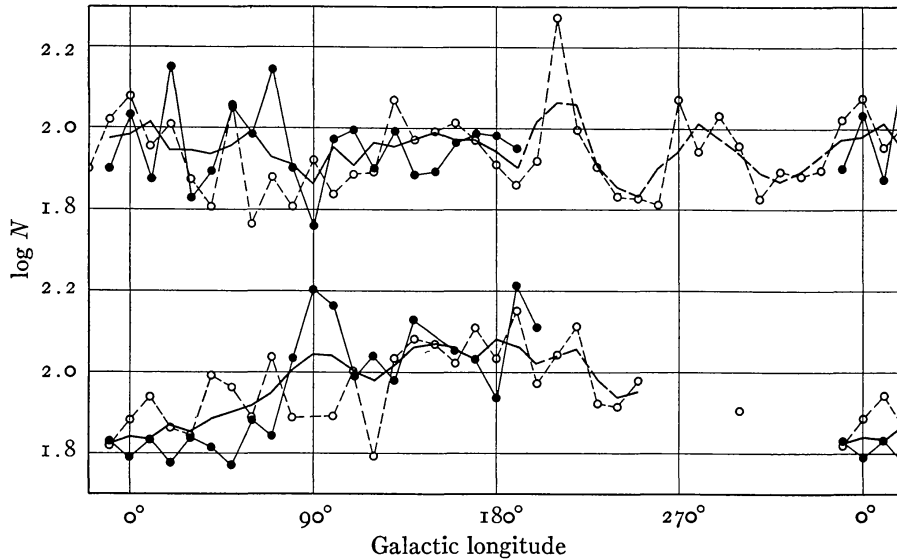


FIG. 4.— $\log N$ as a function of longitude. The upper diagram represents the distribution in zone $\beta = 40^\circ$ to 50° ; the lower, in zone $\beta = 20^\circ$ to 30° . Circles indicate northern latitudes; and disks, southern latitudes. The heavy line represents overlapping means of three successive intervals of longitude. Data from Table X; all values of $\log N$ reduced to the galactic poles by the corrections in Table XII.

refer to flares from the zone of avoidance with their bordering obscuration or to regions beyond the limits of the survey. A single FP plate for a southern field, $\lambda = 290^\circ$, with an abnormal $\log N$, is omitted as uncertain.

The heavy lines in Figure 4 represent overlapping means of three successive values, derived from the combined data for the two hemispheres (full lines) when both are available, and otherwise, for the northern hemisphere alone (dash lines). The zones $\beta = 40^\circ$ to 50° show no conspicuous systematic variations. Certain residual effects might suggest galactic obscuration, but apparent abnormalities do

not in general survive a comparison of similar diagrams for zones 35° to 45° and 45° to 55° .

Zones 20° to 30° exhibit the conspicuous excess in $\log N$ in the direction of the galactic anticenter over those in the direction of the center typical of the galactic belt. Qualitatively the data suggest appreciably greater obscuration in the direction of the center, and, quantitatively, an overcorrection for the latitude effect.

DISTRIBUTION IN LATITUDE

Since longitude effects are not conspicuous in the polar caps, variation with latitude can there be investigated simply by plotting the mean $\log N$ for various latitude zones against the latitudes. A preliminary analysis indicated a definite correlation following the trend of a cosecant law. Attempts were then made to extend the investigation into the low latitudes of the galactic belt. Contours were drawn beyond the borders of the zone of avoidance, purporting to avoid the fringe of local partial obscuration without prejudice to obscuration which might arise from a pervading medium. All fields outside the contours were then used in deriving values of mean $\log N$ for latitude zones within the galactic belt itself. The procedure is admittedly arbitrary and, in fact, selective effects actually appear in the final results. Nevertheless, large areas in the lower latitudes were added in which the trend of the correlation could be examined with some confidence.

The data for both polar caps and galactic belt are listed in Table XI, where $\log N$ is given for successive 10° zones (the two extreme zones range from 0° to 7° and from 78° to 90°). Survey and extra-survey and northern and southern fields are listed both separately and combined. All fields in Tables II and III were used without exception, but numerous survey fields were omitted as indicated in the footnotes. The latitude effect is apparent in both survey and extra-survey fields, but it is more conspicuous in the latter. It seems probable, however, that the most reliable representation is given by the two groups combined.

Figure 5 exhibits all the data for the two hemispheres, separately and combined. The curves for the two hemispheres are in good agreement; they cross and recross, and the greatest differences are at the

extremities where the data are few. The southern point nearest the pole, for instance, depends upon only 14 plates, while the points

TABLE XI*
LOG *N* AS A FUNCTION OF GALACTIC LATITUDE

β	EXTRA-SURVEY			SURVEY			TOTAL			
	<i>n</i>	$\overline{\log N}$	$\bar{\beta}$	<i>n</i>	$\overline{\log N}$	$\bar{\beta}$	<i>n</i>	$\overline{\log N}$	$\bar{\beta}$	O-C†
Northern Hemisphere										
78°-90°...	18	2.010	81.9	19	1.889	82.1	37	1.948	82.0	-0.016
68-77....	45	2.049	72.6	30	1.887	72.0	75	1.984	72.4	+ .026
58-67....	53	1.988	62.2	54	1.881	61.7	107	1.934	61.9	- .011
48-57....	32	2.032	54.1	71	1.892	52.5	103	1.935	53.0	+ .008
38-47....	34	1.873	43.0	72	1.894	42.5	106	1.887	42.7	- .007
28-37....	20	1.906	33.3	58	1.848	32.9	78	1.863	33.0	+ .023
18-27....	14	1.726	23.6	38	1.766	22.8	52	1.755	23.0	+ .024
8-17....	10	1.393	13.0	18	1.611	13.6	28	1.533	13.4	+ .065
0-7....	1	1.660	7.0	1	1.240	5.0	2	1.450	6.0	+0.770
90-0....	227	1.940	54.5	361	1.854	46.7	588	1.887	49.7
Southern Hemisphere										
78-90....	3	2.047	82.0	11	2.039	82.3	14	2.041	82.2	+0.077
68-77....	4	2.092	72.2	17	1.944	72.1	21	1.972	72.1	+ .015
58-67....	15	2.183	62.1	40	1.889	62.4	55	1.969	62.3	+ .023
48-57....	28	1.932	52.9	41	1.897	52.4	69	1.911	52.6	- .015
38-47....	18	1.928	41.9	39	1.868	42.4	57	1.887	42.3	- .005
28-37....	13	1.840	32.8	40	1.766	32.4	53	1.784	32.5	- .052
18-27....	25	1.702	22.7	31	1.721	22.7	56	1.712	22.8	- .016
8-17....	18	1.346	13.1	18	1.570	13.3	36	1.458	13.2	.000
0-7....	4	1.070	5.0	4	1.070	5.0	+0.675
90-0....	124	1.829	39.8	241	1.818	44.4	365	1.822	42.8

* The following survey fields in the galactic belt ($\beta < 40^\circ$) are omitted (in zones 25° , 30° , and 35°) as seriously affected by partial obscuration bordering the zone of avoidance, or used (in the lower zones) as probably free from such obscuration:

- | | |
|--|--|
| $\beta = +35^\circ$, omit $\lambda = 320^\circ-300^\circ$
30, omit 60-90, 310-340
25, omit 60-90, 300-350
20, use 10-50, 110-230
15, use 20-50, 140-220
10, use 30-40, 190-210
+ 5, use 210 | $\beta = -35^\circ$, omit $\lambda = 140^\circ-150^\circ$
30, omit 150, 340
25, omit 140-160, 340-350
20, use 10-30, 70-120, 160-200
15, use 0-10, 60-110, 160-170, 190-200
10, use 70-80, 100-110, 200-210
- 5, use 70, 160-170, 210 |
|--|--|

The two cluster fields at $\beta = +20^\circ$, $\lambda = 150^\circ$ and $\beta = +30^\circ$, $\lambda = 170^\circ$ are also omitted.

† The calculated values are derived from the equation, $\log N = 2.115 - 0.15 \text{ cosec } \beta$.

nearest the galactic plane represent only 2 and 4 plates in the northern and southern hemispheres, respectively.

TABLE XI—Continued

β	EXTRA-SURVEY			SURVEY			TOTAL			
	n	$\overline{\log N}$	$\bar{\beta}$	n	$\overline{\log N}$	$\bar{\beta}$	n	$\overline{\log N}$	$\bar{\beta}$	O—C†
	Combined									
78°-90° ...	21	2.015	81.9	30	1.944	82.2	51	1.973	82.1	+0.009
68-77 ...	49	2.053	72.6	47	1.908	72.0	96	1.982	72.3	+ .024
58-67 ...	68	2.031	62.2	94	1.884	62.0	162	1.946	62.1	+ .001
48-57 ...	60	1.986	53.5	112	1.894	52.5	172	1.926	52.8	- .001
38-47 ...	52	1.856	42.6	111	1.885	42.5	163	1.887	42.5	- .006
28-37 ...	33	1.880	33.1	98	1.814	32.7	131	1.831	32.8	- .007
18-27 ...	39	1.711	23.2	69	1.746	22.8	108	1.733	22.9	+ .003
8-17 ...	28	1.362	13.1	36	1.591	13.5	64	1.491	13.3	+ .028
0-7 ...	1	1.660	7.0	5	1.104	5.0	6	1.197	5.3	+0.706
90-0 ...	351	1.901	49.3	602	1.840	45.6	953	1.862	47.4

The means for the two hemispheres combined (the crosses) are represented with remarkable fidelity from 90° down to about 15° by the smooth curve

$$\log N = 2.115 - 0.15 \operatorname{cosec} \beta. \quad (2)$$

Below 15°, the crosses fall above the curve, a result either of selection or of a failure of the cosecant law. Some further information is furnished by the two triangles at $\beta = 10^\circ.1$ and $14^\circ.9$, which represent means for all plates in the zones 8° to 12° and 13° to 17° on which any nebulae at all could be found, i.e., only the zone of avoidance itself has been excluded, while the fringe of presumably partial obscuration is included in the data.²⁶ Effects of selection should force the triangles below the true relation while possibly forcing the crosses above. It is uncertain how much significance may be attached to

²⁶ The results for all plates on which any nebulae are found for $\beta < 22^\circ$ are as follows:

INTERVAL	n	$\overline{\log N}$	$\bar{\beta}$	O—C	
				$\log N$	β
18°-22°	59	1.593	20.0	-0.083	-3°3
13-17	60	1.425	14.9	- .107	-2.4
8-12	38	1.169	10.1	- .091	-1.0
0-7	14	0.813	5.1	+0.385	+1.5

the fact that the cosecant curve does fall between the crosses and the triangles.

The deviations from the cosecant law, equation (2), given in Table XI, include only one significant residual for the two hemispheres combined exceeding 0.01, namely, +0.024 for the zone 68° to 77°.

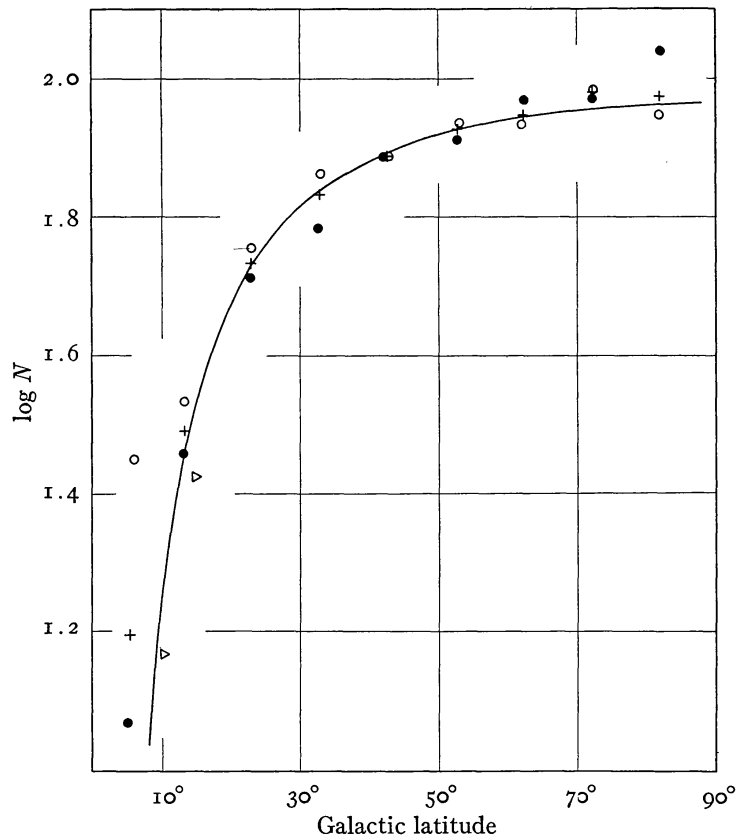


FIG. 5.—Log N as a function of latitude. Data from Table XI. Circles represent northern latitudes; disks, southern latitudes; and crosses, the means. The two triangles indicate supplementary data in low latitudes as described in the text. The curve is the cosecant relation $\log N = 2.115 - 0.15 \operatorname{cosec} \beta$.

Moreover, when the two lowest zones are omitted as uncertain, the systematic deviations of the northern and southern hemispheres from the cosecant law are +0.006 and -0.007, respectively. The systematic difference between the two hemispheres, 0.013, is within the uncertainties of the data. The similarity in the distribution for the two hemispheres is in sharp contrast to previous results. The greatest un-

certainty probably arises from incompleteness in the southern hemisphere, although it may be emphasized that 60 per cent of the southern polar cap and a larger fraction of the galactic belt are included in the survey.

On the assumption of uniform distribution (effects of red shift being ignored), the coefficient in the cosecant law indicates a differential obscuration between 30° and the pole, and hence a total obscuration at the pole, of

$$0.15 \div 0.6 = 0.25 \text{ pg mag.}$$

The optical thickness of the obscuring medium, from pole to pole, is therefore 0.5 mag., with an estimated uncertainty of the order of 0.1 mag. In view of the close agreement between the two hemispheres, the sun is presumed to be near the median plane of the obscuring medium.

Two other recent investigations of the latitude effect lead to results of the same general nature. In 1931, E. F. Carpenter²⁷ reported that the nebulae "show, with some scatter, essentially uniform surface brightness approximately down to latitude 30° or 40° , where a diminution sets in which at 20° amounts to nearly half a magnitude." Actually, the cosecant law indicates differential obscuration at 20° of about 0.48 mag., and in the high latitudes the obscuration is so inconspicuous that Carpenter's results cannot be considered as inconsistent.

In 1932, P. van de Kamp²⁸ fitted cosecant relations to the distribution in latitude of the Harvard survey of bright nebulae and of Fath's counts in Selected Areas. The optical thickness, from pole to pole, was found to be of the order of 0.8 mag. from the former and 1.4 mag. from the latter, as compared to 0.5 mag. from the present data. His analysis indicated, however, conspicuously greater obscuration in the southern hemisphere, and accordingly he located the

²⁷ *Publications of the American Astronomical Society*, 7, 25, 1931. The results are reported in an abstract and are not given in detail, hence they cannot be compared with Wirtz's earlier investigation (*Meddelanden från Lunds Astron. Observatorium*, Ser. II, No. 29, 1923) which indicated no conspicuous correlation between surface brightness and latitude. J. Dufay (*Comptus rendus*, 196, 101, 1933) has also discussed the material, finding a positive effect but of a smaller amount.

²⁸ *Astronomical Journal*, 42, 97, 1932.

sun well to the north of the median plane of the obscuring medium, in marked contrast to the present results, which indicate no appreciable difference.

The obscuration for the most part is general rather than selective, since no conspicuous relation has been detected between latitude and color excess of nebulae. For instance, the group of spirals including IC 1303, at $\beta = +7^\circ$, has been investigated by the method of exposure-ratios and, although the data are by no means precise, it seems probable that the color excess, if present, does not differ by more than 0.2 mag. from that exhibited by nebulae in high latitudes. The cosecant law indicates a differential absorption of the order of 1.8 pg mag. between the field and the pole, and hence color excess of any amount might be expected up to the maximum of 0.9 mag. corresponding to Rayleigh scattering.

The large color excesses of globular clusters measured by Stebbins²⁹ refer for the most part to objects actually within the zone of avoidance and presumably affected by the isolated clouds which define the zone. This, together with results from nebular distribution, suggests that the cosecant law in equation (2) may refer to material other than that concentrated in the great clouds. A strict interpretation of the cosecant law leads, of course, to a widely extended uniform layer of diffuse matter such as Eddington and others have discussed at length. The law was derived from mean points representing all available fields in each latitude zone. In the polar caps this appears to be unobjectionable, but in the low latitudes of the galactic belt the systematic effect in longitude (Fig. 4) must be taken into account. Since the mean points fall close to the curve while the residuals are distributed harmonically, the excess of obscuration in the direction of the galactic center more or less balances the deficiency in the opposite direction. This fact invites speculation and suggests the possibility of an extensive flattened cloud of thinly distributed material, oriented on the galactic plane, in which the sun is located near the median plane but between the center and the outer rim. Similar clouds are actually seen as dim lens-shaped silhouettes ex-

²⁹ *Proceedings of the National Academy of Sciences*, **19**, 222, 1933. Stebbins' results, if referred to a uniform layer of diffuse material, would give a color excess at $\beta = 7^\circ$ of about 0.65 mag. for distances corresponding to those of the globular clusters.

tending for many degrees along the Milky Way. Such speculations will have no significance, however, until the very complex data on local obscuration in low latitudes are more carefully explored and untangled. They are mentioned merely to emphasize the fact that, while a uniformly diffused medium may be postulated for statistical purposes, the present data on nebular distribution cannot be considered as inconsistent with the assumption that the major part of

TABLE XII
LATITUDE CORRECTIONS, REDUCING LOG N TO THE GALACTIC POLE

β	$\Delta\beta^*$	β	$\Delta\beta^*$	β	$\Delta\beta^*$
76°-90°	0.00	31°	0.14	17°	0.36
66-90	.01	30	.15	16	.39
59-65	.02	29	.16	15	.43
55-58	.03	28	.17	14	.47
51-54	.04	27	.18	13	.52
48-50	.05	26	.19	12	.57
45-47	.06	25	.20	11	.64
42-44	.07	24	.22	10	.71
40-41	.08	23	.23	9	.81
38-39	.09	22	.25	8	0.93
37	.10	21	.27	7	1.08
35-36	.11	20	.29	6	1.28
34	.12	19	.31	5	1.57
32-33	0.13	18	0.34		

* $\Delta\beta = 0.15 (\operatorname{cosec} \beta - 1)$.

galactic obscuration arises from isolated clouds rather than from a uniform medium.

Latitude corrections, $\Delta\beta$, derived from the cosecant law, are listed in Table XII. When added to $\log N$, they reduce the counts to the galactic poles. The equivalent obscuration in photographic magnitudes is $\Delta\beta/0.6$. For statistical purposes the corrections are probably significant down to 15°, but below 40° the longitude effect introduces an artificial scatter which should be considered in interpreting results.

The latitude effect necessitates a revision of the reductions and analyses—the last step in the series of approximations. The correction for atmospheric extinction is not affected. The corrections for quality and exposure time have been redetermined, but since the revisions are of minor significance and do not materially affect the

final results, they will not be considered in detail. The application of the latitude corrections to the analysis of distribution in longitude has been anticipated, and there remains only the effect on the general distribution. The corrected distribution is shown in Figure 6, which is similar to Figure 3, but with $\log N$ reduced to the poles and the irregularities exhibited in greater detail.

The range in $\log N$ formerly defined as normal distribution is divided into a central range only half as large (maximum numbers about twice the minimum), bordered by moderate excesses and deficiencies. The mean $\log N$ for the polar caps is 1.965, and normal distribution, indicated by small crosses, is now defined $\log N = 1.82-2.11$. Moderate deviations are represented by small disks for excesses ($\log N = 2.12-2.26$) and small circles for deficiencies ($\log N = 1.67-1.81$). The remaining symbols, for large deviations, are the same in both maps and have the same significance. In Figure 6, however, the blank fields in the zone of avoidance are omitted.

The large circles emphasize the effects of local obscuration and the map represents a second approximation to their delineation. The failure of the cosecant law, i.e., the longitude effect in the galactic belt, is indicated by the frequency of large excesses in the low latitudes opposite the galactic center. Normal distribution, even when so narrowly defined, still dominates the polar caps and sweeps down to the Milky Way between the great flares in the zone of avoidance. Nearly 65 per cent of the fields in the polar caps are normal, and the others are about equally divided between excesses and deficiencies.

FREQUENCY DISTRIBUTION OF $\log N$

The significance of normal distribution is emphasized by the frequency distribution of $\log N$. This has been investigated in two steps. In the first, only fields in the polar caps were used, uncorrected for latitude; in the second, latitude corrections were applied, and all fields down to and including 15° were used, excepting those obviously affected by obscuration bordering the flares in the zone of avoidance. The data³⁰ are given in Tables XIII and XIV, where numbers of sur-

³⁰ Two fields only were omitted in the polar caps (Table XIII), the cluster field $\beta = +55^\circ$, $\lambda = 10^\circ$, and the heavily obscured survey field $\beta = -40^\circ$, $\lambda = 140^\circ$. The fields in Table XIV are essentially those used in Table XI for $\beta \geq 15^\circ$.

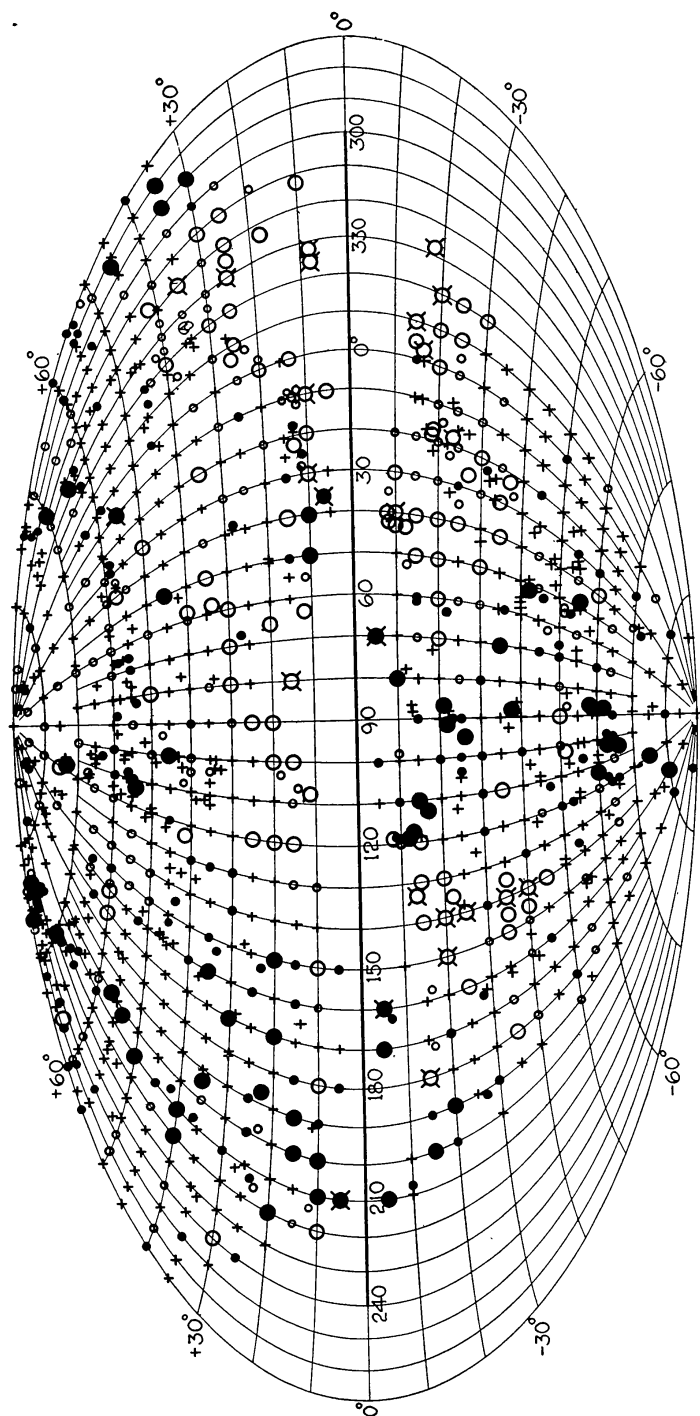


FIG. 6.—Distribution of extra-galactic nebulae when observed data are corrected for the latitude effect. Small crosses represent normal distribution ($\log N = 1.82-2.11$); small disks and circles, moderate excesses ($\log N = 2.12-2.26$) and deficiencies ($\log N = 1.67-1.81$); large disks and circles, considerable excesses ($\log N = 2.27-2.56$) and deficiencies ($\log N = 1.37-1.66$), with crosses added for $\log N > 2.56$ and $\log N < 1.37$. Fields with no nebulae are omitted.

vey and extra-survey fields are listed both separately and combined for successive intervals of 0.05 in $\log N$. Fields falling on divisions are equally divided between the adjacent intervals. The last three columns in each table represent smoothed frequencies derived from overlapping means of three successive counts.

TABLE XIII
FREQUENCY DISTRIBUTION OF $\log N$
($\beta \geq 40^\circ$)

$\log N$	COUNTS			OVERLAPPING MEANS OF THREE		
	Survey	Extra-survey	Total	Survey	Extra-survey	Total
1.40-1.45...				0.3		0.3
.45-.50...	1		1	1	0.7	1.7
.50-.55...	2	2	4	2.2	2.2	4.3
.55-.60...	3.5	4.5	8	6.2	2.7	8.8
.60-.65...	13	1.5	14.5	10.8	5	15.8
.65-.70...	16	9	25	18.3	5.3	23.7
.70-.75...	26	5.5	31.5	32.7	8.5	41.2
.75-.80...	56	11	67	41.2	9.2	50.3
.80-.85...	41.5	11	52.5	47.8	14.7	62.5
.85-.90...	46	22	68	46.4	19.5	65.8
.90-1.95...	51.5	25.5	77	50.8	25.2	76
1.95-2.00...	55	28	83	45	27	72
2.00-.05...	28.5	27.5	56	32.7	28.3	61
.05-.10...	14.5	29.5	44	20.3	26.3	46.7
.10-.15...	18	22	40	14	23.3	37.3
.15-.20...	9.5	18.5	28	11.8	16.8	28.7
.20-.25...	8	10	18	6.7	11.8	18.5
.25-.30...	2.5	7	9.5	4	6.5	10.5
.30-.35...	1.5	2.5	4	1.7	4.8	6.5
.35-.40...	1	5	6	0.8	2.8	3.7
.40-.45...		1	1	0.3	2	2.3
.45-.50...					0.7	0.7
.50-.55...		1	1		0.3	0.3
2.55-2.60...					0.3	0.3
Total....	395	244	639	394.9	243.9	638.9

The data are exhibited graphically in Figure 7 (for the polar cap alone) and in Figure 8 (for the longer list in Table XIV). Figure 7 is included to emphasize the fact that the complication of latitude corrections in Figure 8 does not affect the general order of the results, while the additional data appreciably smooth the shapes of the curves.

The outstanding feature in Figure 7 is the displacement of the

extra-survey group with respect to the survey, which was mentioned earlier in the discussion. The discrepancy is slightly reduced in Figure 8, but remains conspicuous.

TABLE XIV
FREQUENCY DISTRIBUTION OF LOG N CORRECTED FOR LATITUDE EFFECT

LOG N	COUNTS			OVERLAPPING MEANS OF THREE		
	Survey	Extra-survey	Total	Survey	Extra-survey	Total
1.15-1.20...					0.3	0.3
.20-.25...		1	1		0.7	0.7
.25-.30...		1	1		0.7	0.7
.30-.35...					0.5	0.5
.35-.40...		0.5	0.5	0.3	0.3	0.7
.40-.45...	1	0.5	1.5	0.3	0.5	0.8
.45-.50...		0.5	0.5	0.7	0.7	1.3
.50-.55...	1	1	2	2	1.2	3.2
.55-.60...	5	2	7	5.3	3.8	9.2
.60-.65...	10	8.5	18.5	12.3	7	19.3
.65-.70...	22	10.5	32.5	21.8	9.5	31.3
.70-.75...	33.5	9.5	43	33.7	10.7	44.3
.75-.80...	45.5	12	57.5	45.2	13	58.2
.80-.85...	56.5	17.5	74	57.2	16.5	73.7
.85-.90...	69.5	20	89.5	64.2	19.7	83.8
.90-1.95...	66.5	21.5	88	69.8	28.2	98
1.95-2.00...	73.5	43	116.5	67.2	33.2	100.3
2.00-.05...	61.5	35	96.5	58.2	38	96.2
.05-.10...	39.5	36	75.5	47.8	35.5	83.3
.10-.15...	42.5	35.5	78	33	32.2	65.2
.15-.20...	17	25	42	26.2	27.5	53.7
.20-.25...	19	22	41	15.3	19.3	34.7
.25-.30...	10	11	21	10.5	12.2	22.7
.30-.35...	2.5	3.5	6	5.2	8.2	13.3
.35-.40...	3	10	13	2.4	5.2	7.7
.40-.45...	2	2	4	3	4.3	7.3
.45-.50...	4	1	5	2.5	1.3	3.8
.50-.55...	1.5	1	2.5	2	0.7	2.7
.55-.60...	0.5		0.5	0.7	0.3	1.0
2.60-2.65...				0.2		0.2
Total....	587	331	918	587.0	331.2	918.1

The curve for the survey fields in Figure 8 is fairly symmetrical about the most frequent value $\log N = 1.925$, while that for the extra-survey fields exhibits an appreciable skewness with the peak about $\log N = 2.03$. The skewness suggests effects of selection which, since it is shared by fields centered both on co-ordinates and on nebulae, must be referred to abnormal distribution rather than to the sup-

position, once current, that small nebulae tend to cluster around large nebulae. Minor selective effects are clearly evident and most of the skewness can be traced to about fifty apparently abnormal

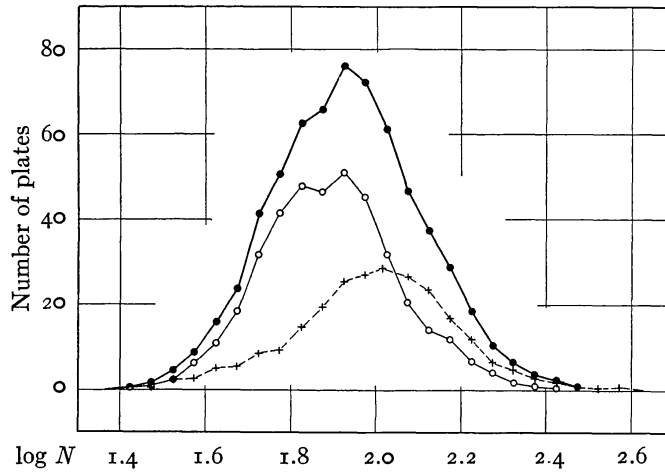


FIG. 7.—Frequency distribution of $\log N$ for fields in the polar caps with no correction for latitude effect. Data from Table XIII. Circles represent the 395 survey fields; crosses, the 244 extra-survey fields; disks, the combined data, 639 fields.

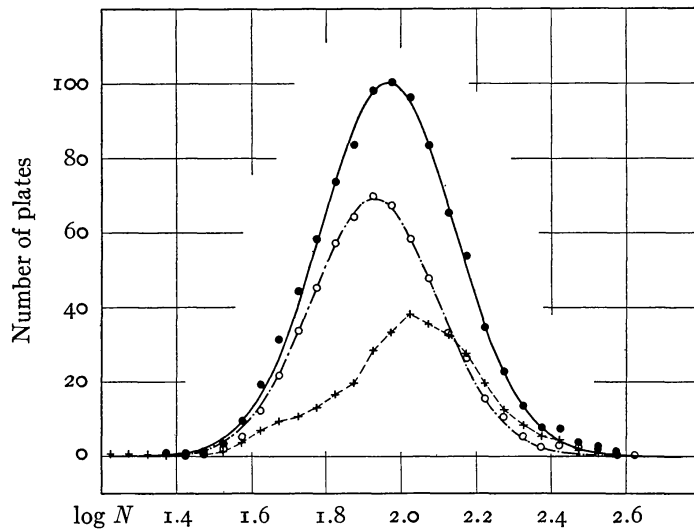


FIG. 8.—Frequency distribution of $\log N$ reduced to the galactic poles. Data from Table XIV. Crosses represent the 331 extra-survey fields; circles, the 587 survey fields; disks, the combined data, 918 fields. The smooth curves through the survey fields and the combined data (the two upper curves) are normal error-curves adjusted to the points.

fields. Attempts to improve the data involve rather arbitrary methods and criteria, however, and eventually the two groups, survey and extra-survey, were simply combined. This procedure gives the broad features of the frequency distribution as indicated by the sum total of the data without prejudice to the minor deviations which more detailed analysis may ultimately disentangle.

The curve represents a random distribution of $\log N$ —the percentage deviations from the geometrical mean of the counts are distributed according to the normal error-curve. This probably corresponds to what may be termed a normal distribution of the counts themselves, which, since they range upward from a finite lower limit, may be expected to exhibit a positive skewness in their frequency distribution. The transformation to logarithms, which range in theory from minus to plus infinity, offers a possibility of representation by the Gaussian curve which is actually realized by the data to a very close approximation. This feature characterizes all the data from the regions of normal distribution, including the original uncorrected counts as well as those reduced to the standard conditions, and in addition the counts by Curtis and the Harvard survey of the brighter nebulae. The approximately Gaussian distribution of $\log N$ may therefore be considered an observed characteristic of nebular distribution except in so far as modified by local galactic obscuration.

A detailed analysis of the curves, including the influence of reductions, the calculation of numerical characteristics, possible interpretations, etc., is reserved for a more extended discussion. Meanwhile, it may be mentioned that the upper curve in Figure 8, representing the most extensive list of data, has a range in $\log N$ of the order of 1.0 (1.5–2.5 when seven fields are omitted from the total of 918) and a “probable error” of the order of 0.12 for a single field, including errors of observation and of reduction. The mode and mean are about equal at $\log N = 1.965$ (92 nebulae), and the standard samples are derived from counts averaging about fifty nebulae per field in the polar caps. The dispersion in any other random collection of homogeneous samples should be comparable with these results when adjusted for relative richness of the samples. Moreover, since the average richness depends upon volumes of space and not upon angu-

lar areas represented by samples, the statement may be expected to apply to counts of bright nebulae over large areas as well as counts of faint nebulae over small areas.

The Harvard survey, for instance, includes about 738 nebulae in the polar caps brighter than 13.0 pg mag. The caps can each be very simply divided into say 40 equal areas by dividing each 10° zone, e.g., $40^\circ-50^\circ$, $50^\circ-60^\circ$, etc., into the appropriate number of blocks and combining the odd bits left over. In an actual trial, 8 of the 80 fields were blank, and in general the frequency of the fields diminished as the number of nebulae increased. Nevertheless, when logarithms were used, a fairly symmetrical distribution was suggested with a peak at about 0.90 and a probable error of the order of ± 0.28 . When adjacent pairs of areas were combined and only 40 areas were used for the distribution, no field was blank and the approximation to a Gaussian curve was much improved. The most frequent $\log N$ was then about 1.10 and the probable error about $\times 0.24$.

Curtis' counts, including 177 fields in the polar caps, 1 of which is blank, show the same features—a conspicuous positive skewness in the distribution of numbers but an approximately Gaussian distribution of logarithms with the peak at about $\log N = 1.30$ and a probable error of the order of ± 0.20 . The approximation is closer when Curtis' counts are corrected for varying quality and exposure times—a conclusion derived from an examination of the plates made possible through the courtesy of the Director of the Lick Observatory. The most frequent $\log N$ is then about 1.40 and the probable error of the order of ± 0.18 .

Fath's counts in Selected Areas include 55 fields in the polar caps, 2 of which are blank. They do not conform so well, but the failure can be attributed to the wide range in the limiting magnitudes of the plates. A forced representation of the data suggests a most frequent $\log N$ of about 0.95 with a probable error of the order of 0.30.

CLUSTERS OF NEBULAE

The great clusters, recognized as such from casual inspection, have not been included in the discussions. They are relatively rare; perhaps twenty are recognized at the present time, and most of them have been photographed at Mount Wilson. If included in Figure 8

they would in general fall beyond $\log N = 2.40$ and increase the slight excess over the error-curve which is already apparent. The excess may indicate unrecognized clusters, but at least part of it refers to the artificial scatter introduced by the reductions.

The usage of the term "cluster" is quite arbitrary, ranging from the conservative practice which applies the name only to the great conspicuous examples to the other extreme in which almost any grouping is glorified by the title. The writer is obviously a conservative, and the following remarks apply only to the great aggregations of several hundred members each. Three such clusters in the northern sky—those in Virgo and Coma, both well known, and the new cluster in Corona Borealis found on the survey plate at $\beta = +55^\circ$, $\lambda = 10^\circ$ —are especially important, since they are extraordinarily rich and at widely different distances. For these reasons they afford excellent opportunities for statistical investigations of characteristics which vary with distance. Each contains between five hundred and one thousand members of various types, and their distances are of the order of 2, 14, and 40 million parsecs, respectively.

Clusters were found in only two other survey fields, namely, $\beta = +20^\circ$, $\lambda = 150^\circ$ (Gemini) and $\beta = +30^\circ$, $\lambda = 170^\circ$ (Cancer). Thus, from the survey fields, the frequency is uncertainly estimated as of the order of 3 clusters per 590 fields, or 1 per 100 square degrees. Mayall and the writer found two faint clusters in a survey covering 50 square degrees in the Virgo cluster, and Baade reports two typical clusters and one doubtful case from a survey of 103 square degrees in Ursa Major made with the 1-m reflector at Hamburg. These scanty data suggest a frequency of the order of perhaps 1 cluster per 50 square degrees.³¹ On the assumption of an average population of four to

³¹ Results of neither survey are published. Baade's data were communicated privately to the writer with permission to mention them. The clusters in Gemini and in Cancer (the latter found independently by Carpenter at the Steward Observatory) and one of the clusters in Ursa Major (found independently at Mount Wilson) are described in *Mt. Wilson Contr.*, No. 427; *Astrophysical Journal*, **74**, 43, 1931.

The Harvard survey of the Virgo cluster (*Harvard Bulletin*, No. 865, 1929) calls attention to five independent groups in the area of about 125 square degrees covered by the survey. None of these is within the smaller area of the Mount Wilson survey, and only two, Harvard groups *c* and *d*, approach the dignity of clusters as the term is here used. On plates with the 60-inch reflector at Mount Wilson, these fields lead to $\log N = 2.31$ and 2.37, respectively, and hence are borderline cases.

five hundred nebulae per cluster, about 10 per square degree may be assigned to the great clusters recognized as such with large reflectors,³² or about 1 per cent of all nebulae to the limits involved. When groups are included, the clustering tendency becomes more appreciable and significant, especially when considered in connection with the systematic advance in average type from the dense clusters to the random nebulae.

On the grand scale, however, the tendency to cluster averages out. The counts with large reflectors conform rather closely with the theory of sampling for a homogeneous population. Statistically uniform distribution of nebulae appears to be a general characteristic of the observable region as a whole.

PART II. NUMERICAL CALIBRATION OF THE COUNTS

The discussion thus far has been concerned with relative numbers of nebulae per field. The reduction of the numbers per unit area to a definite limiting magnitude requires a correction for distance from the optical axis, here called the "coma factor," and the determination of the limiting magnitude for a particular exposure time.

COMA FACTOR

Distortions of stellar images, the coma effect in particular, increase rapidly with distance from the optical axes of short-focus reflectors. This circumstance enhances the difficulties of distinguishing nebulae from stars and renders the threshold of identification a function of distance from the axis, the counts of nebulae tending to thin out toward the edges of the plates. The effect can be determined by combining a sufficient number of fields to smooth out accidental irregularities in distribution and plotting numbers of nebulae in concentric rings against the radii of the rings.

For the immediate purpose, however, an even simpler procedure is sufficient. In addition to counts over the entire plates, Tables I–III list, in the columns headed *I*, the numbers of nebulae in central cir-

³² Clusters on plates other than systematic surveys cannot be used with the same confidence since they represent a certain degree of deliberate selection. It may be significant, however, that 10 additional clusters appear on such Mount Wilson plates whose combined areas total about 400 square degrees in the regions free from the more conspicuous effects of local obscuration.

cles with radii of $18.75 \text{ mm} = 5'$ for the 5×7 -inch plates with the 100-inch and $15.25 \text{ mm} = 6.9'$ for the 4×5 -inch plates with the 60-inch. If the definition were uniform, the ratio of the number of nebulae on the entire plate to the number in the inner circle should be the same as the ratio of the areas. Actually the former ratio is the larger, since the numbers fall off in the outer regions; and in order to equalize them the counts for the entire plate must be multiplied by a factor which is the quotient of the two ratios. In this manner the counts may be reduced to a uniform definition over the entire plate equal to the average definition within the central circle. The coma factor, of course, must be derived for each telescope separately. The procedure assumes that the relative numbers of bright and faint nebulae are statistically uniform; but it amounts to something more than merely deriving the numbers per unit area from the inner circles alone, since all plates³³ with six or more nebulae are included, whether in the polar caps or the galactic belt.

The essential data are summarized in Table XV, which includes both the coma factor adopted for each telescope and the area factor. The area factors are merely the reciprocals of the effective areas of the plates expressed in square degrees, by means of which the numbers of nebulae per plate are reduced to numbers per square degree. In deriving the coma factors, outer circles with radii double those of the inner were used as controls. The corresponding counts are omitted from Tables I–III, but the sums are given in Table XV where n refers to the number of fields, N_T to the sums of the counts over the entire plate, I to the counts in the inner circle, II to those in the larger circle less the inner circle, $I+II$ to the counts in the larger circle complete. The data from Tables I, II, and III are tabulated both separately and combined. Ratios were first calculated for each quality class in order to examine the possibility of systematic variations with quality, but differences were not conspicuous (except for the class FP where the data are too meager for reliable results) and were ignored in the final determinations.

The fields in Table III, centered on selected nebulae, required special treatment, since it was necessary to eliminate the central nebulae and correct for the areas they covered. This was accomplished with

³³ Except the cluster fields.

the aid of the quantities ab , the products of the two diameters of the nebulae, listed in the table, by means of which the areas were estimated as fractions of the inner circles. The values of ab are not precise and are often unduly large in order to avoid uncertainties which might arise from small detached outliers of the later-type spirals.

TABLE XV
COMA FACTOR

	n	N_1	I	II	N_1/I	N_1/II	$N_1/I+II$
100-Inch							
Survey.....	340	12,761	1379	3411	9.254	3.741	2.664
Fields.....	55	4,412	464	1179	9.509	3.711	2.669
Nebulae.....	93	5,671	658	1516	8.619	3.741	2.609
Total.....	488	22,844	2501	6116	9.134	3.735	2.651
60-Inch							
Survey.....	332	11,051	1547	3152	7.144	3.506	2.352
Fields.....	34	1,857	244	500	7.611	3.714	2.496
Nebulae.....	142	6,017	752	1708	8.001	3.523	2.446
Total.....	508	18,925	2543	5360	7.442	3.531	2.395

	100-Inch	60-Inch
Adopted value of N_1/I	9.15	7.40
Ratio of areas.....	17.71	14.56
Coma factor.....	1.936	1.968
Area factor.....	2.590	1.647

Ratios for the plates centered on nebulae are more uncertain than the others, but it is interesting to note that the values from the two telescopes are one above and one below the mean ratios from the other plates. For the two telescopes combined, the ratio from the plates centered on nebulae is very closely the same as that from plates centered without reference to nebulae. This appears to dispose of the

opinion, once current, that small nebulae tend to cluster around large nebulae.

NEBULAR MAGNITUDES AT THE THRESHOLD OF IDENTIFICATION FOR HOUR EXPOSURES

Limiting photographic magnitudes on the international scale of nebulae at the threshold of identification for hour exposures with each telescope are given in Table XVI. The internal agreement is good, since each value represents the mean of several selected plates for a field rich in nebulae. The more important systematic scale error, however, is less certain. Only two standard sequences, the Pole and S.A. 57, were used for the comparisons, and only the latter

TABLE XVI
THRESHOLD MAGNITUDES OF NEBULAE FOR ONE-HOUR EXPOSURES

60-INCH			100-INCH		
Field	$m_{(thres.)}$	Plates	Field	$m_{(thres.)}$	Plates
Ursa Major.....	19.3	6	Coma.....	20.05	5
Perseus.....	19.5	2	Perseus.....	20.1	3
Cor. Borealis.....	19.4	3	Cor. Borealis....	19.9	4
Virgo Field.....	19.5	4	Gemini.....	20.0	2
Mean.....	19.4	Mean.....	20.0

was available for direct use with the 100-inch. The two standard sequences were compared directly down to about 19.0 by the writer with the 60-inch. The scale in S.A. 57 was extended to 19.5 and fainter with the 100-inch by Baade, who has very kindly permitted the use of his unpublished results.

With the aid of these standards, sequences of stellar magnitudes were established in each field listed in Table XVI which were considered reliable to 19.0 or 19.5 and could be extrapolated with reasonable confidence to 20.0 or thereabouts. Magnitudes of small faint nebulae were then derived from long-exposure schraffierkassette plates taken with the 100-inch, with images about 1 mm square, which to limits ranging from 19.0 to 19.3 are considered to be of the same order of accuracy as the stellar magnitudes. These values are the standard nebular magnitudes upon which the results in Table

XVI are ultimately based, although the latter in general depend upon extrapolations.

With the 60-inch, standard magnitudes were available for threshold images on direct exposures ranging up to about forty-five minutes and, with slight extrapolations, up to the full hour. With the 100-inch, however, even thirty minutes' direct exposure generally involved some extrapolation, and estimates of threshold magnitudes for hour exposures depended upon the relation between limiting magnitude and exposure time for the particular observing conditions. The latter relation assumes such importance that an extensive collection of data was assembled from plates by several different observers, using different telescopes and observing conditions. These data all led to the same conclusion, namely, that for small surface images at the threshold of fully developed Eastman 40 plates, exposed from about ten minutes to two hours, the simple reciprocity law very closely represents the observations.³⁴ The Schwarzschild exponent is not less than unity and occasionally, possibly under optical conditions of sky fog, may be greater than unity. The reciprocity law in its appropriate form,

$$\text{Threshold mag.} = 2.5 \log E + C ,$$

was therefore used to extrapolate the observed threshold magnitudes on direct exposures from fifteen to forty-five minutes to corresponding magnitudes for one-hour exposures.

Another and independent approach to the subject is offered by a relation previously derived³⁵ between surface brightness and diam-

³⁴ The data were derived from plates under the following conditions: (a) 100-inch with schraffierkassette, images 2 mm and 1 mm square, exposures 6-180 minutes, magnitudes from Selected Area No. 57. Plates by the writer. (b) 10-inch Cooke refractor with schraffierkassette, images 2 mm and 1 mm square, exposures 4-110 minutes, magnitudes from N.P.S. Plates by Willis and by Christie. (c) 5-inch Ross camera extra-focal, with excellent uniform images 1.1 mm and 0.45 mm in diameter, exposure 10-120 minutes, magnitudes from N.P.S. Plates by Willis.

The investigation consisted in identifying the faintest star images seen with certainty and comparing the known magnitudes with the logarithms of the exposure times. Each group, representing a particular size of image with a particular instrument, was examined separately and no group suggested a Schwarzschild exponent less than unity. A detailed discussion of the investigation will be given later.

³⁵ *Mt. Wilson Contr.*, No. 453; *Astrophysical Journal*, 76, 106, 1932.

eters of threshold images on Eastman 40 plates. For very small images the total magnitude is independent of the size; for very large images the surface brightness is independent of the size. The observed relation is a smooth transition between these limiting conditions and was determined numerically for the express purpose of deriving statistical values for limiting magnitudes of nebulae in the present investigation.

The data for large images were derived from extra-focal exposures ranging from one to ninety minutes and were originally reduced to a uniform exposure time by means of the assumption that tripling the exposure increases the limit of the plate by 1 mag. This assumption is now believed to be wrong for surface images, and, in fact, an inspection of residuals in the previous discussion indicates some systematic deviations in the direction anticipated. The data have been reduced on the assumption of a strict reciprocity law, and new curves derived accordingly. The major features are unaffected, although the numerical values are slightly modified and the former systematic discrepancy between the two reflectors appreciably reduced. Systematic deviations related to exposure times are still apparent but opposite in direction to those found on the assumption previously used. It appears, therefore, that the particular data are best represented by an intermediate form of the law of blackening and that mean values from the two curves will not be greatly in error.

This conclusion was confirmed by an inspection of a large number of plates of qualities E and GE, which indicated that the average diameters of threshold images of the nebulae actually identified are of the order of 4'' and 5'' for the 100-inch and 60-inch, respectively. The corresponding total magnitudes for hour exposures, as derived from the curves of surface brightness revised by the reciprocity law, are 20.06 and 19.50, and 19.72 and 19.30 from the curves as originally published. The differences for the two instruments are only 0.34 and 0.2 mag., respectively. The mean values, 19.89 and 19.40, should be of the proper order at least, and are in fact in fair agreement with the values in Table XVI. Another way of stating the agreement is that the mean values correspond to diameters of 4''.25 and 5''.5 from the reciprocity-curve and of 3'' and 4''.5 from the original curve for the two reflectors, respectively, and that these values are all of the gen-

eral order of the limiting diameters of nebulae actually identified. In view of the uncertainties in estimating diameters of threshold images, the agreement is all that can be expected, and the values in Table XVI are used in the discussions which follow.

The fact that the adopted values are a half-magnitude and more brighter than the limiting magnitudes for star images on good plates suggests that many nebulae below the threshold of identification are recorded on the plates and that their numbers may be comparable with those of the nebulae actually identified. A comparison of eight

TABLE XVII
NUMBERS OF NEBULAE PER SQUARE DEGREE TO
DEFINITE LIMITING MAGNITUDE

	100-Inch	60-Inch
$\log N$	1.965	1.805
\log Coma factor	0.287	0.294
\log Area factor	0.413	0.217
$\log N$ (sq. deg.)	2.665	2.316
m (threshold)	20.0	19.4

two-hour exposures with the 100-inch with one-hour exposures of the same fields with the 60-inch amply confirmed this expectation, indicating about 300 unrecognizable nebulae on the 60-inch plates in addition to 395 which had previously been identified. The available data are insufficient for a comprehensive discussion of the subthreshold images, but for the immediate purpose such a discussion is unnecessary, provided a definite threshold is consistently maintained and the corresponding limiting magnitude fairly established. The data emphasize, however, the importance of personal equations and their calibration.

NUMBERS OF NEBULAE PER SQUARE DEGREE TO
DEFINITE LIMITING MAGNITUDES

The counts can now be reduced to numbers of nebulae per square degree. The mean $\log N$ for the 100-inch, from the upper curve in Figure 8, is 1.965, and for the 60-inch is 0.16 less, or 1.805. When the logarithms of the coma and area factors (Table XV) are added, the results are as shown in Table XVII.

Assuming uniform distribution and ignoring effects of red shifts, we have from these results the relation

$$\begin{array}{r} \log N_m = 0.6m - 9.335 \text{ (100-in.)} \\ \quad \quad \quad \underline{9.324 \text{ (60-in.)}} \\ \quad \quad \quad 9.33 \text{ (mean)} \end{array}$$

EFFECT OF THE RED SHIFT

Regardless of the unit of distance, the red shift is approximately indicated by the relation³⁶

$$\log v = 0.2m + 0.5,$$

where v is the red shift expressed as a velocity in km/sec. and m the photographic magnitude corrected for the effect of the shift. At $m = 20$, the velocity is of the order of 30,000 km/sec. and $d\lambda/\lambda$ about 10 per cent. Some simple approximations already published³⁶ indicate that the effect on the photographic magnitudes at such distances is very appreciable and cannot be ignored.³⁷

The approximations were based on two assumptions. The first, that $d\lambda/\lambda$ is constant throughout the spectrum, is established within the uncertainties over an observed range between the emission lines normally at 5007 and 3727 Å and is generally accepted by those who interpret the shifts as Doppler effects. The second assumption is that nebular luminosity approximates black-body radiation, with effective spectral type, G3d, temperature, and color (for nebulae showing small shifts) similar to those of the sun. The normal observed spectra are similar to the solar spectrum as far as the small scale permits comparison, and for the brightest nebulae, the greater the scale the closer the analogy, except for the widened lines in the nebular spectra. It is possible that the mixture of stars supposed to exist in nebulae may seriously affect the assumed distribution of

³⁶ *Mt. Wilson Contr.*, No. 427; *Astrophysical Journal*, **74**, 43, 1931. For the present purpose, the significant quantity is $d\lambda/\lambda$. From the relation above, $\log d\lambda/\lambda = 0.2m - 5$ approximately.

³⁷ J. Stobbe (*Astronomische Nachrichten*, **243**, 53, 1931) has constructed intensity-curves for black-body radiation at various temperatures, as affected by red shifts of various amounts. These indicate the effect on the bolometric intensity at any wavelength and furnish data for following the effect up to the photographic magnitudes.

energy, and there are some reasons for believing that even the nearer nebulae in high latitudes exhibit an appreciable color excess. For the present, however, we may use the assumption as a first approximation.

On these two assumptions red shifts produce redistributions of intensity which can be represented by new black-body curves corresponding to lower temperatures, and hence to later spectral types. The decrease in ν introduces an increment to the bolometric magnitude that can be followed in a purely empirical manner up to the photographic magnitude, which it enters in a magnified form. De-

TABLE XVIII
OBSERVED PHOTOGRAPHIC MAGNITUDES OF NEBULAE CORRECTED
FOR EFFECT OF RED SHIFT

Obs.	Corr.	Obs.	Corr.	Obs.	Corr.
22.0	21.15	19.5	19.22	17.0	16.90
21.5	20.83	19.0	18.78	16.0	15.94
21.0	20.45	18.5	18.32	15.0	14.96
20.5	20.05	18.0	17.85	14.0	13.97
20.0	19.65	17.5	17.38		

tails will be found in the previous publication,³⁸ where Δm_{pg} are tabulated for various values of $d\lambda/\lambda$.

Table XVIII, giving corrected photographic magnitudes corresponding to various observed magnitudes, is derived from these data. The corrected limiting magnitudes for one-hour exposures with the 100-inch and 60-inch reflectors are 19.6 and 19.1, respectively. The revised relation between numbers of nebulae and limiting magnitude is

$$\begin{aligned} \log N_m &= 0.6m - 9.095 \text{ (100-in.)} \\ &\quad \underline{9.140 \text{ (60-in.)}} \\ &= 9.12 \text{ (mean)} \end{aligned}$$

where m now refers to the corrected apparent magnitude. Unless the estimated effects of red shifts are greatly in error, the relation may be expected to hold generally.

³⁸ *Mt. Wilson Contr.*, No. 427; *Astrophysical Journal*, 74, 43, 1931.

The Harvard survey of brighter nebulae leads to a fairly symmetrical frequency distribution of $\log N$ in the polar caps around a mode at about $\log N = -1.46$ per square degree.³⁹ The corresponding limit of survey is $(9.12 - 1.46) \div 0.6 = 12.8$, which is very close to the limit assigned by the authors of the survey.

The Harvard counts of fainter nebulae have not been sufficiently calibrated for a comparison to indicate more than the general order of the agreement. The most extensive data⁴⁰ are given in the form of mean values, $\log N$ per square degree, reduced to a uniform limiting stellar magnitude of 18.2, for successive zones of latitude 10° wide. One hundred and forty-five fields in the polar caps are included, each representing 9 square degrees. The mean $\log N$ for this extensive material is 1.26, or 1.30 if the latitude corrections for the middle of each zone are added. The latter value corresponds to a corrected limiting magnitude of 17.4, or an observed magnitude of about 17.5, which is of the general order to be expected for a limiting stellar magnitude of 18.2.

Other fragmentary data are fairly consistent, although no great weight can be assigned to the results. For instance, unpublished counts of about two thousand nebulae in twenty fields with the 10-inch Cooke refractor at Mount Wilson indicate an average of about three nebulae per square degree to a limiting magnitude of about 16.0. These are round numbers, but the calculated limit is 16.0, plus a correction of less than 0.1 mag., which indicates the order of the agreement.

Seares's⁴¹ analysis of Fath's counts in Selected Areas indicates an average of about 14 nebulae per square degree over the polar caps—55 fields are in these regions—representing a calculated observed limit of about 17.2 as compared with Seares's estimates of 18.6 for the average stellar limiting magnitude. The apparent discrepancy is due largely to the personal equation in the counts since an inspec-

³⁹ A mean value can be used if proper allowance is made for the Virgo cluster. Thus, about 625 nebulae are scattered over the 14,600 square degrees in the polar caps (less the area of the Virgo cluster), or approximately 1 nebula per 23.5 square degrees. $\log N$ is thus of the order of -1.37 and the resulting m of the order of $(9.12 - 1.37) \div 0.6 = 12.9$.

⁴⁰ *Proceedings of the National Academy of Sciences*, **19**, 389, 1933.

⁴¹ *Mt. Wilson Contr.*, No. 297; *Astrophysical Journal*, **62**, 168, 1925.

tion of the plates clearly indicates the very conservative criteria used in the identification of nebulae.

Curtis' counts can be used with confidence only when fully calibrated, but a preliminary comparison of fields included in the Mount Wilson collection suggests an agreement in the general order of the results which detailed investigation may be expected to confirm.

The nebulae increase with limiting magnitude at such a rate that near the galactic poles they equal the stars in number⁴² at about 21.25 mag. Since this limit represents rather closely the threshold of identification that can be reached with long exposures under good conditions with the 100-inch, the equality offers an interesting measure of the greatest penetrating power available at the present time. $\log N$ at the limit is about 3.25, corresponding to about 1780 nebulae per square degree, or 75,000,000 over the sphere. The number actually observable is reduced by local obscuration, but the reduction is more than compensated by the numbers registered below the threshold of identification. It is interesting also that the number is only a fraction, possibly one-third, of the number that would be expected in the absence of fading due to red shifts over and above the fading due to distance alone.

DENSITY OF NEBULAR DISTRIBUTION

Since the density of nebulae in space is merely the numbers divided by the volume,

$$\log \rho = \log N - \log V ;$$

and since for the entire sphere, in nebulae per cubic parsec,

$$\begin{aligned} \log N &= 0.6m - 9.12 + 4.62 , \\ &= 0.6m - 4.50 ; \end{aligned}$$

and

$$\begin{aligned} \log V &= \log \frac{4}{3} \pi + 3 \left(\frac{m - M + 5}{5} \right) , \\ &= 0.6m - 0.6M + 3.62 , \end{aligned}$$

⁴² *Mt. Wilson Contr.*, No. 301; *Astrophysical Journal*, 62, 320, 1925.

it follows that

$$\log \rho = 0.6M - 8.12 ,$$

where M is the mean absolute photographic magnitude of nebulae.

The density is expressed in this form because M is still uncertain, owing largely to uncertainties in the scale of apparent magnitudes. The value⁴³ $M = -13.8$, derived from Holetschek's visual magnitudes corrected by a color index, gives $\log \rho = -16.40$. Another value, $M = 14.5$, giving $\log \rho = -16.82$, was derived for isolated nebulae by H. Knox-Shaw⁴⁴ and has since been used by Shapley.⁴⁵ The latter value was based upon the Harvard magnitudes of bright nebulae, which were derived from direct comparisons with star images on focal exposures, and hence are subject to possible scale errors of the kind exhibited in an exaggerated form by the Harvard magnitudes of globular clusters. Discrepancies of this order will continue to be current until a reliable system of photographic magnitudes is available, derived from large uniform images comparable for both stars and nebulae. Such a program is under way at Mount Wilson, involving extra-focal exposures and the schraffierkassette with various telescopes, and until the necessary data are available, either here or elsewhere, there is little point in enlarging the discussion.

MASSES OF NEBULAE

A revision of the data on the masses of nebulae is possible and may have some significance since the derivation of the density of matter in space is only slightly affected by uncertainties in the absolute magnitudes. The most hopeful present prospect of deriving masses appears to be Öpik's assumption that, on the average, the mass is a constant multiple of the luminosity,

$$\text{Mass} = b \times \text{Luminosity}.$$

The factor b can be evaluated from masses of particular nebulae as indicated by spectrographic rotation, and then applied to the mean

⁴³ *Mt. Wilson Contr.*, No. 427; *Astrophysical Journal*, **74**, 43, 1931.

⁴⁴ *Monthly Notices of the Royal Astronomical Society*, **93**, 304, 1933.

⁴⁵ *Proceedings of the National Academy of Sciences*, **19**, 591, 1933.

luminosity of nebulae in general. Reliable data on rotations share with the magnitude scale the distinction of being the most pressing immediate need in the general field of nebular investigations. Such data are restricted at present to the three nebulae M 31, M 33, and NGC 4594, in addition to the galactic system itself; and in each case the evaluation of the factor b is subject to uncertainties from other sources. Two of the three nebulae are among the brightest known, and hence a simple mean of the masses cannot represent the nebulae in general. The factor b , or some equivalent, must be introduced, and hence it is important to estimate the order of the factor. The uncertainties are so great, however, that the discussion will be restricted to simple estimates of the general order, with no claim to precision.

Messier 31.—No revision of the mass-luminosity relation is available for this spiral, although it is hoped that continued spectrographic observations of the clusters scattered throughout the nebula may contribute information concerning the outer regions which can be added to the rotational data already available for the nuclear region. The greatest uncertainty in the factor b arises from the necessity of extrapolating the mass from the nuclear region actually observed to the entire nebula, together with uncertainties in the magnitudes. The difficulties are discussed in a former publication⁴⁶ where a tentative value of the factor, 5.5, is estimated for mass and luminosity expressed in terms of the sun as the unit.

Messier 33.—The distance and the luminosity are fairly well known, as is also the radial velocity of NGC 604, a bright patch of emission nebulosity near the major axis and about $700''$ from the nucleus. The bright lines in NGC 604 have been measured with moderately large dispersion, and the velocity, -270 km/sec., is probably certain within 10 km/sec. A new value for the velocity of the nucleus has been derived by Humason from several plates, one with relatively large dispersion. This value,⁴⁷ -320 km/sec., is probably correct within 20 km/sec., and agrees with those for M 31 and its

⁴⁶ *Mt. Wilson Contr.*, No. 376; *Astrophysical Journal*, **69**, 103, 1929.

⁴⁷ This represents a revision, based upon new data, of the value -330 , given in the catalogue of velocities (*Publications of the Lick Observatory*, **18**, 1932). The unpublished results were privately communicated to the writer with permission to use them.

companions in reflecting the rotation of the sun around the galactic center.

The differential velocity of NGC 604, 50 km/sec., when corrected for tilt of the plane of the spiral, gives a rotational velocity of 67 km/sec., which is uncertain by perhaps half its value. Nevertheless it represents a decided improvement on the former value⁴⁸ and indicates a revised mass of the order of $9 \times 10^8 \odot$, which is more consistent with the other nebulae. The photographic absolute magnitude is of the order of -13.9 , hence the luminosity is about $7 \times 10^7 \odot$, and the factor b , about 13.

NGC 4594.—The distance as indicated by the red shift is of the order of 2,000,000 parsecs, subject to uncertainties arising from the unknown peculiar motion. The rotation is measured out to about two minutes of arc from the nucleus, where it reaches 330 km/sec., and hence the contribution of the luminosity from the outer unobserved regions is unimportant. The mass is estimated as of the order of $3 \times 10^{10} \odot$, although some questionable assumptions are introduced concerning the nature of the rotation. The apparent photographic magnitude is given in the Harvard survey as 8.0, but extra-focal and schraffierkassette plates with the 5-inch and 10-inch cameras indicate that it is probably a magnitude fainter,⁴⁹ and hence that the absolute luminosity is about $2 \times 10^9 \odot$. The factor b is then about 15.

The three values of b —5, 13, and 15—suggest a factor of the order of 10 for nebulae in general. The mean mass is then of the order of 6×10^8 or $10^9 \odot$, depending on the adoption of -13.8 or -14.5 as the mean absolute magnitude.

DENSITY OF MATTER IN SPACE

The mean mass of nebulae, in terms of the sun as the unit, is

$$\log \text{Mass} = \log b + 0.4(5.7 - M) .$$

⁴⁸ The mass of M 33 was formerly estimated on the basis of a nuclear velocity of -70 km/sec., a value recognized as very uncertain since it was derived from a single plate of very low dispersion.

⁴⁹ The precise value is uncertain owing to uncertainties in the comparison stars. If the *HD* magnitudes are used the nebula is about 9.8, nearly the same magnitude as that of the star BD $-11^{\circ}3342$, listed in the *HD* as G0, 9.3 visual and 9.9 photographic.

Hence, from the previous expression for the density of nebular distribution,

$$\log \rho = 0.2M + \log b - 5.84 ,$$

where the density is expressed in suns per cubic parsec. In grams per cubic centimeter,

$$\log \rho = 0.2M + \log b - 28.02 .$$

Since $\log b$ is of the order of unity and M is variously estimated as -13.8 to -14.5 ,

$$\log \rho = -29.8 \text{ or } -29.9 ,$$

with an uncertainty probably less than 0.5. The round number -30 is convenient and within the uncertainties. It has been widely used of late, although the justification has been largely convenience rather than quantitative investigation. The value is of the order of ten times greater than the first tentative estimate put forward in 1926, and it is believed that further significant revisions of the order of the density must await more extensive investigations of spectrographic rotations.

The discussion, of course, ignores the existence of internebular matter, the density of which, even in an optimal form, might be several thousand times greater without introducing appreciable absorption. Since absorption depends upon the state of the material (the density for large meteorites, for instance, might surpass that of the galactic system without introducing appreciable obscuration), upper limits can be assigned to the density of internebular space only from dynamical considerations.

CARNEGIE INSTITUTION OF WASHINGTON
MOUNT WILSON OBSERVATORY
August 1933